ISSN Application No. 21797

Journal of Hydropower and Civil Engineering

Volume No. 9

Issue No. 3

September - December 2025

ENRICHED PUBLICATIONS PVT. LTD

S-9, IInd FLOOR, MLU POCKET,
MANISH ABHINAV PLAZA-II, ABOVE FEDERAL BANK,
PLOT NO-5, SECTOR-5, DWARKA, NEW DELHI, INDIA-110075,
PHONE: - + (91)-(11)-47026006

Journal of Hydropower and Civil Engineering

Aims and Scope

Journal of Hydropower and Civil Engineering envisage to publishes best of reviews and researches within the broad field of civil engineering which include construction management, geotechnical engineering, transportation engineering, concrete technology, and very importantly the water engineering

Journal of Hydropower and Civil Engineering

Journal of Hydropower and Civil Engineering

(Volume No. 9, Issue No. 3, September - December 2025)

Contents

Identification Of Regional Frequency Model For Rainfall Based On Spatial Clustering In Lower Tapi Basin, India

Garima Nagpal[1], Dr. P.L.Patel[2]

[1]M. Tech Scholar, Centre of Excellence on 'Water Resources and Flood Management', Sardar Vallabhbhai National Institute of Technology Surat, Surat - 395007, India

[2]Professor, Department of Civil Engineering, SardarVallabhbhai National Institute of Technology Surat, Surat - 395007, India

Email: garima.alpha@gmail.com, plpatel@ced.svnit.ac.in

ABSTRACT

The hydrologic frequency analysis is a base for hydraulic design and water resources management. When the hydrologic data is scarce, regional frequency is adopted to enhance the quality of quantiles predictions from the at site analyses. In regional frequency analysis, the selection of appropriate probability distribution has been important to estimate the quantiles accurately. The candidate probability distributions used in this technique are generalized extreme value (GEV), generalized logistic (GLO), generalized Pareto (GPA), log normal (LN), and Pearson type III (PE3). The present study has been applied to lower Tapi basin for analysis of rainfall extremes. The available rainfall data gaps in the daily time series were first filled by inverse distance weighting (IDW) method. The regional model has been developed using L-moments approach while using data for annual maximum rainfall series for the period of 33 years (1973-2005) at eleven stations in the basin. Discordancy measures were used for the initial screening of sites data to check for the inconsistencies, and test was used for outliers present in the sample data. The three regions were formed using agglomerative hierarchical clustering technique, and plotting a dendrogram for eleven rain gauge stations. The Monte Carlo simulations were undertaken to test the heterogeneity of the region by fitting Kappa distribution using regional average L-moments ratios. The heterogeneity measures reported for the three regions were 0.845, -1.086 and -0.141 respectively for region I, II, and III. The trend of the annual maximum series at all stations were determined using Mann-Kendall and innovative trend analysis methods, and it was observed that six stations reported a decreasing trend, while five stations reported an increasing trend. The Z-statistic test has been used for the three regions to select the best fitted probability distribution, and subsequently, for prediction of regional quantiles. It has been found that GPA, GLO and PE3 probability distributions best represented regions I, II and III respectively, based on minimum Z-statistic values which were worked out to be 1.071, 0.310, and 0.160 respectively. The development of regional model would be helpful in prediction of at-site quantiles for different return periods based on the problem under consideration.

Keywords:Regionalization, L-moment approach, Heterogeneity measure, Monte Carlo simulations, Trend analysis, Lower Tapi basin

1. Introduction

The extreme rainfall event causes severe damages to lives and properties of the inhabitants in the catchment.In recent years, it has been observed that the extreme rainfall events can also lead to

flooding. With the use of frequency analysis of extreme rainfall events, the frequency of occurrence of rainfall events can be predicted for different return periods. The estimation of rainfall events of various return periods are required for the development of vulnerable maps at regional scales.Various distribution have been used in the estimation of extreme rainfall events for at-site data, however, they were proved not so accurate in estimation in regional scales. Hosking and Wallis (1993) described the classical procedure of regional frequency analysisof annual maximum series (AMS)of hydrological data using L-moments,and proved that the L-moments approach performsbetter than the conventional moments, as former considers both the physiographic and statistical parameters. Trefry (2004) found the application of partial duration series model in regional frequency analysis by adjusting the quantiles estimates of AMS series using empirical factor.After Hosking (1993), other researchers like Kjeldsen (2002), Trefry (2005), Hussain and Pasha (2008), Hussain (2011), Akhtar (2003), Rahman (2013), Wong and Tung (2013) and othersfollowed classical regional frequency analysis for the analysis of hydrological data.To find the erroneous site, the conventional method of discordancy measures was proposed by Hosking and Wallis (1993).Saf (2009) found the gaps in the classical theory of discordancy measures by comparing classical method with the robust method which uses minimum covariant determinant. The homogeneity of pooling stations is the basic requirement of the regional frequency analysis as explained by Dalrymple(1960). Castellarin (2008) assessed the presence of inter-site correlations, and their impacts on the traditional statistical method of assessing heterogeneity measure as proposed by the Hosking and Wallis (1993, 1997).For the development of regional model, the rain gauge stations are clustered into the regions using agglomerative hierarchical clustering, adopted byBothale(2014) in which mean annual precipitation and site elevation were taken as attributes.Some cities in the Tapi basin like Suratcity, are vulnerable to floods and heavy rainfall events, and, therefore, estimation of extreme events of various return period is required for managing the flood and developing the vulnerable maps in the region. The objective of the present study is to analyze the frequency of extreme rainfall events at regional level by filling the missing rainfall data, checking the discordant site, forming the homogeneous regions and fitting suitable distributions for the identified homogeneous regions. The developed regional scale models for homogeneous regions may be useful in predicting the extreme rainfall events in the regions which, in turn, would be useful in developing the vulnerable maps and managing the flood events.

2. Study Area and Data Availability

The study area includes the lower Tapi basin which is lying betweenGidhade gauging station to the Arabian Sea, and covers an area of 10,395 sq. km. Thelower Tapi basin covers different percentage of area in Dhule, Khargaon, Surat, and Bharuch districts. The data available for this study are daily rainfall series and their latitude-longitude at eleven rain gauge stations,namely, Surat, Kamrej, Mangrol, Olpad,

Bodhan, Kadod, Kathor, Kholavad, Puna, Mandvi and Kakrapar. The data used in the study were taken from the government agencieslike India Meteorological department (IMD) and State Water Data Centre (SWDC), Gandhinagar, Gujarat. The data used in the regionalization is daily annual maximum rainfall series for the period (1973-2005). The index map of the lower Tapi basin is shown in Fig.1.

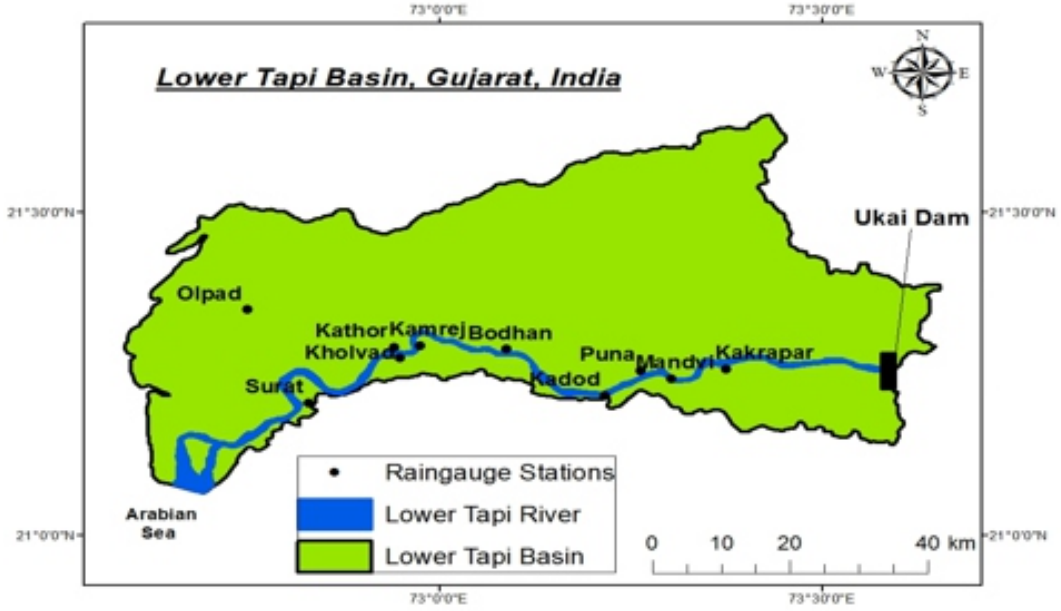

3. Methodology

3.1 Missing data analysis

The available time series for rainfall were partly missing atfew stations for certain periods. It was customary to estimate missing rainfall before moving to regional frequency analysis. The 'Inverse distance weighing (IDW) method'as given in the paper of Chen and Liu (2012), has been used in the estimation of missing rainfall, for present study is expressed as:

$$\hat{R}_p = \sum_{i=1}^{N} w_i R_i \qquad (1a)$$

$$w_i = \frac{d_i^{-\alpha}}{\sum_{i=1}^{N} d_i^{-\alpha}} \qquad (1b)$$

where, $\hat{R}_p$ means the unknown rainfall data, w_i means the weighting of each rainfall stations, d_i means the distance from each rainfall stations to the unknown site, α means the power which has been taken 2 in this study.

3.2 L-moments

Among various methods available for regional frequency analysis,L-moments has been chosen as the best approach for regionalization. As unlikeother methods it considers, both statistical and

physiographical characteristics of the data. When the data series is arranged in ascending order, where jis the order of the data series and n is the total number of data in the series,the L-moments can be defined as a linear combination of probability weighted moments (PWMs)

$$\beta_r = \frac{1}{n}\sum_{j=1}^{n}\frac{(j-1)(j-2)\dots\dots(j-r)}{(n-1)(n-2)\dots\dots(n-r)}x_{j:n} \qquad (2)$$

The first four sample L-moments are given as

$$\lambda_1 = \beta_0 \qquad (3a)$$

$$\lambda_2 = 2\beta_1 - \beta_0 \qquad (3b)$$

$$\lambda_3 = 6\beta_2 - 6\beta_1 + \beta_0 \qquad (3c)$$

$$\lambda_4 = 20\beta_3 - 30\beta_2 + 12\beta_1 - \beta_0 \qquad (3d)$$

The L-moments can be made independent of units of measurement, called L-moment ratios,and are given as

$$t = \frac{\lambda_2}{\lambda_1} \qquad (4a)$$

$$t_3 = \frac{\lambda_3}{\lambda_2} \qquad (4b)$$

$$t_4 = \frac{\lambda_4}{\lambda_2} \qquad (4c)$$

$$t_r = \frac{\lambda_r}{\lambda_2} \qquad (4d)$$

The L-moments ratios for the population is represented by τ_r instead of t_r

3.3 Discordancy Measures

The available data are required to be screened for their appropriateness using Discordancy measures as proposed by Hosking and Wallis (1997). The discordancy measures represents the difference between the L-moment ratios of a site and the average L-moment ratios of a group of sitesin the region. The discordancy measure for the i^{th}

$$D_i = \frac{1}{3}N(u_i - U)^T A^{-1}(u_i - U) \qquad (5)$$

The station can be defined in a three-dimensional space using L-moment ratios t_2, t_3 and t_4 If N is number of rain gauge stations present in a region, then u_i is transpose vector of the L-moment ratios at i^{th} station, and can be expressed as,

$$u_i = (t_2, t_3, t_4)^T \quad (6)$$

The unweighted group average U of the vector and a matrix A of sum of squares and cross products are defined as

$$U = \frac{1}{N}\sum_{i=1}^{N} u_i \quad (7)$$

$$A = \sum_{i=1}^{N} (u_i - U)(u_i - U)^T \quad (8)$$

The station can be flagged as discordant, if its discordancy measure is greater than the critical value.

3.4 Regional Homogeneity Test

In general, Generalized Pareto distribution, Generalized extreme-value distribution, Generalized logistic distribution, Pearson type III distribution, Lognormal distribution, Wakeby distribution, Kappa distribution are the frequently used distributions in the regional frequency analysisCunnane (1989). In regionalization method, called index flood procedure which is proposed by Hosking and Wallis (1993), the stations with frequency distributions that are identical, apart from a station-specific scale factor, are clubbed together such that they satisfy the condition of homogeneity. Grouping of stations may be based on several characteristics such as latitude, longitude, elevation, and mean annual precipitation. The agglomerative hierarchical clustering has been used to club the stations that begins with singleton clusters andproceeds by merging smaller clusters into larger ones successively. This process is repeated until a single cluster is left. The entire process may be represented in a nested sequence, called the dendrogram, which shows the relationship of the clusters at various steps of the process. A distance measure has been used in present study to evaluate the dissimilarity between any two cluster centroids, or feature vectors.

To ensure the regional homogeneity, Hosking and Wallis (1993) suggested a test statistics as Heterogeneity measure (H). TheL-moments approach being used to check the heterogeneity measure,is based on the theory that all stations in the region have the same population. For a homogenous region, the heterogeneity measure compares the between-site variations in sample L-moments for the group of sites. The homogenous regions can be examined using a Monte Carlo simulation procedure which is accomplished by fitting a four parameter Kappa distribution to the regional average L-moment ratios, Dupuis and Winchester (2007). The regions herein are synthetically generated using 500 simulations, and assumed to be homogenous and have the same characteristics as the real region. The statistics H for

the homogeneity of a region can be estimated as

$$H = \frac{(observed\ dispersion) - (mean\ of\ simulations)}{(standard\ deviation\ of\ simulations)} \quad (9)$$

$$H_k = \frac{(V_k - \mu_v)}{\sigma_v}, \qquad k = 1,2,3 \quad (10)$$

Here, V is the weighted standard deviation of the at-site sample L-CVs (t), i is the number of sites in a region. The V2 computes at-site dispersion of sample L-moments based on L-CV and L-skew and V3, which measures the at-site dispersion of sample L-moments based on L-skew and L-kurtosis. Theparameters μ_v and σ_v are the mean and standard deviation of the synthetic counterparts of V respectively. According to Hosking and Wallis (1993), a region is considered to be acceptably homogenous if $H_k < 1$, , possibly heterogeneous if $1 \leq H_k \leq 2$, and definitely heterogeneous if $H_k \geq 2$.

3.5 Selection of best fit probability distribution

In regional frequency analysis, a single frequency distribution is fitted to data from several sites of a region which would give quantile estimates for each site. The objective of regional frequency analysis is to define accurately a robust common distribution which best fits to the data of all sites in the homogeneous region. To determine an appropriate distribution for regional quantile estimation, a goodness of fit measure was introduced by the Hosking and Wallis (1997) for the three parameter distributions, called Z-statistics which measures the difference between the theoretical L-kurtosis of the fitted distribution to the regional average L-kurtosis of the observed data. The Z-statistics or goodness of fit measure for any three parameter distribution is given as:

$$Z^{DIST} = \frac{(\tau_4^{DIST} - t_4^R + B_4)}{\sigma_4} \quad (11)$$

τ_4^{DIST} is the theoretical L-kurtosis for the candidate distribution, t_4^R is the regional average L-kurtosis weighted by record length, $B_4$is the bias correction used for t_4; and σ_4 is the estimate of the standard deviation of t_4^R obtained from the repeated simulation of a homogenous region whose sites have the candidate frequency distribution and record lengths as that of observed data. Selection of best fit distribution is followed by the estimation of regional quantile parameters, namely, location, scale and shape. The estimated parameters are used to calculate quantile estimates for different return periods or, conversely the return period corresponding to a given extreme values.

4. Results and Discussions

The frequency analysis requires data of minimum 30years, after filling the gaps in the daily rainfall. The daily annual maximum rainfall of eleven stations are analyzed for the period 1973-2005 and their

statistical parameters are described in Table 1.

Table 1: Statistical properties of data used in present study

Station No.	Name of Station	Mean (mm)	Coefficient of Variance (mm^2)	Coefficient of Skewness	Coefficient of Kurtosis
1	Surat	158.94	3769.55	0.57	8.18
2	Kamrej	164.44	8161.76	1.34	1.65
3	Mangrol	164.67	6272.25	0.92	-0.78
4	Olpad	121.29	4176.63	1.71	-1.51
5	Bodhan	164.81	7025.98	0.86	1.67
6	Kadod	166.6	4748.23	0.49	8.25
7	Kathor	134.32	4105.81	0.99	1.41
8	Kholavad	128.16	4272.12	2.75	0.24
9	Puna	170.68	3373.59	0.78	2.08
10	Mandvi	145.12	4070.65	0.49	1.98
11	Kakrapar	139.2	3609.55	0.75	2.47

4.1 Recognition of Discordant sites

The L-moment ratios t (L-C_v), t_1 (L-C_s), and t_4 (L-C_k) of all the eleven stations each having 33 years of data are calculated, and 'u' vector of L-moment ratios are determined. The computed values of discordancy measure for all the eleven sites are shown in Table 2.

Table 2: Computed values of L-moment ratios and discordancy measures for rain gauge stations

Station No.	Name of Station	n_i	t	t_3	t_4	D_i
1	Surat	33	0.22	0.094	0.088	0.564
2	Kamrej	33	0.295	0.284	0.161	0.843
3	Mangrol	33	0.265	0.219	0.168	0.68
4	Olpad	33	0.272	0.298	0.142	0.75
5	Bodhan	33	0.285	0.22	0.088	0.602
6	Kadod	33	0.237	0.114	0.085	0.378
7	Kathor	33	0.263	0.221	0.15	0.209
8	Kholavad	33	0.238	0.373	0.302	2.435
9	Puna	33	0.189	0.07	0.097	1.436
10	Mandvi	33	0.253	0.137	0.051	0.425
11	Kakrapar	33	0.242	0.214	0.072	1.676

The critical value of discordancy measure for 11 stations is 2.632, which is higher than theDi value of all eleven stations. Hence, all the sites can be considered suitable for frequency analysis.

4.2 Homogeneity Test

Agglomerative hierarchical clustering has been used in present study for forming homogeneous regions for regional frequency analysis using complete linkage method and the clubbed stations are presented in the form of a dendrogram.

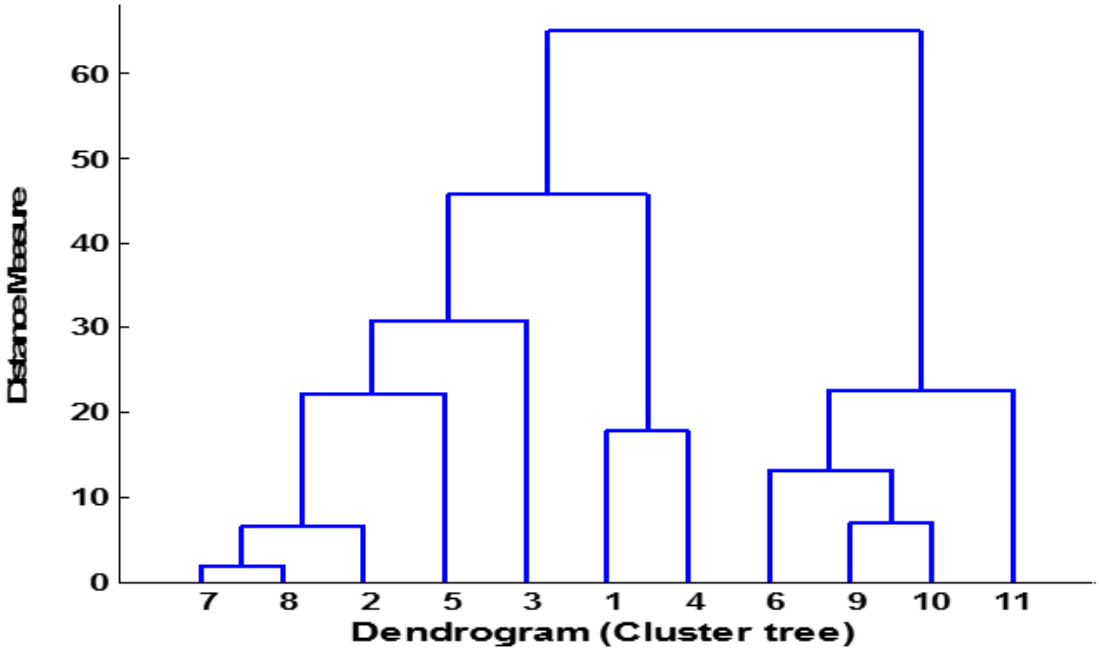

Figure 1.1:Dendrogram (Cluster tree) for 11 rain gauge stations

Optimum number of clusters werecalculated by plotting the number of clusters formed with respect to their resulted fusion level. Cluster I contains the stations 6, 9, 10, 11; Cluster II contains the stations 7, 8, 2, 5; Cluster III contains the stations 1, 4 and Cluster IV contains only station 3. As Cluster IV has only one station, it is not included in foregoing analysis, as regional model developed using one station only cannot depict the behavior of a region with accuracy.To test the homogeneity of the formed clusters, the four parameter Kappa distribution has been fitted to regional average L-moment ratios (1, τR, τ3R, τ4R) of all the clusters, and 500 simulations were generated using Monte Carlo simulation such that generated realizations of each region were having same number of sites as in the original clusters. Four parameters of Kappa distribution ξ (location), α (scale), and k, h (shape) parameters were found for the three clusters using trial and error method are described in Table 3.

Table 3: Parameters of Kappa distribution for homogeneous regions

Cluster	$\ddot{e}_1$	$\ddot{e}_2$	$\hat{o}_3$	$\hat{o}_4$	$\acute{A}$	$\hat{i}$	k	h
I	155.399	35.559	0.134	0.076	93.5	96.125	0.33	0.656
II	147.931	40.348	0.274	0.175	60.439	98.368	0.356	-0.073
III	140.115	33.97	0.196	0.115	69.937	90.359	0.551	0.14

The heterogeneity measures H_1, H_2 and $H_3$for all three clusters I, II and III were estimated as described earlier. The estimated values of heterogeneity measures included in Table 4 for all the clusters. As the estimated values of heterogeneity measures are less than their critical value (< 1.0), hence all the selected clusters can be considered as homogeneous.

Table 4: Heterogeneity measures for homogeneous regions

Cluster	H_1	H_2	H_3
I	0.845	-1.272	-1.774
II	-1.086	-1.736	-1.03
III	-0.141	0.51	0.488

4.3 Z-Statistics Measures

The fit of a probability distribution can be treated as satisfactory, if $|Z^{DIST}| \leq 1.64$ at 5% significance level as given by Hosking and Wallis (1997). The selected probability distributions which are satisfying the above mentioned criteria are tabulated in Table 5 for the three regions. Table 5shows that the selection of best fit distribution for regions I, II and III can be judged by the minimum value of ZDIST-statistics which were obtained as 1.071 for generalized Pareto distribution of region I, 0.310 for generalized logistic distribution of region II, and 0.160 for Pearson type III distribution of region III.

Table 5: Z-statistics test for homogeneous regions

Region	Distribution	t_4^R	$\hat{o}_4^{DIST}$	B_4	$\acute{o}_4$	Z^{DIST}	$\lvert Z^{DIST} \rvert$
I	GPA	0.076	0.043	0.002	0.028	-1.071	1.071
II	GEV	0.175	0.2	-0.063	0.03	-1.293	1.293
	GLO	0.175	0.229	-0.063	0.03	-0.31	0.31
III	GEV	0.115	0.161	-0.026	0.04	0.495	0.495
	GLO	0.115	0.199	-0.026	0.04	1.437	1.437
	GPA	0.115	0.075	-0.026	0.04	-1.683	1.683
	PE3	0.115	0.135	-0.026	0.04	-0.16	0.16
	LN	0.115	0.153	-0.026	0.04	0.284	0.284

4.4 Development of regional model

The regional model has been developed by finding regional parameters for the three regions I, II, and III corresponding to their selected best fit distributions. The developed regional models can be expressed in terms of return period T, by taking the inverse of the cumulative distribution function or can be expressed in terms of frequency factor K_T for the non- invertible probability distributions.

For region I, corresponding to GPA distribution having parameters ξ = 0.4176, α = 0.8899 and k = 0.5280, the regional model is represented as

$$\frac{I_T}{\bar{I}} = \xi + \frac{\alpha}{k}(1 - T^{-k}) \tag{12}$$

For region II corresponding to GLO distribution having parameters ξ = 0.8825, α = 0.2382 and k = -0.2741, the regional model is represented as

$$\frac{I_T}{I} = \xi + \frac{\alpha}{k}[1 - (T-1)^{-k}] \tag{13}$$

For region III corresponding to PE3 distribution having parameters α = 2.8371, β = 0.2704 and ξ = 0.2329, the regional model is represented as

$$\hat{x}_T = \hat{\beta}\hat{\alpha} + \hat{\xi} + K_T\sqrt{\hat{\beta}^2\hat{\alpha}} \tag{14}$$

5. Conclusions

The main objective of this study was to analyze the data for the development of regional model for extreme events of different return periods.The following conclusions can be drawn from foregoing studies:

a) The missing rainfall for available rain gauge stations have been completed using IDW method.

b) The discordancy measures has been undertaken for the available rain gauge site, and it is found that all the available sites are suitable for regional frequency analysis.

c) The existing sites in the study have been clustered in three homogeneous regions using the method of Agglomerative hierarchical clustering.

d) For the homogenous regions, the best fit distributions have been identified using ZDIST- statistics which are 1.071 for Generalized Pareto distribution for region I, 0.310 for generalized logistic distribution of region II, and 0.160 for Pearson type III distribution of region III. The estimated parameters of the identified distributions have been used for computation of rainfall of different return periods.

References

Bothale, R., and Katpatal, Y. (2014). Spatial and statistical clustering based regionalization of precipitation and trend identification in Pranhita catchment, India. International Journal of Innovative Research in Science, Engineering and Technology, 3, pp. 12557-12567.

Chen, F-W., and Liu, C-W.(2012) Estimation of the spatial rainfall distribution using inverse distance weighting (IDW) in the middle of Taiwan.Paddy and Water Environment 10.3 (2012): 209-222.

Chow, V. T., Maidment, D. R., and Mays, L. W. (1988).Applied hydrology, McGraw-Hill International, New York.

Cunnane, C., 1989: Statistical distributions for flood frequency analysis. World Meteorological Organization. Operational Hydrology Report No. 33, WMO Publ. No. 718, Geneva.

Dupuis, D.J., and Winchester, C. (2007).More on the four-parameter kappa distribution.Journal of Statistical Computation and Simulation 71(2007): 99-113.

Kjeldsen, T.R., Smilthers, J.C., and Schulze, R.E. (2002) Regional flood frequency analysis in the KwaZulu-Natal province, South Africa, using index-flood method.Journal of Hydrology 255 (2002):194-211.

Hamed, K. and Rao, A. R. (1999), Flood Frequency Analysis, CRC press U.S.A.

Hosking, J.R.M., and Wallis, J.R. (1993).Some statistics useful in regional frequency analysis.Water Resources Research 29(2): 271-281.

Hosking, J.R.M., and Wallis, J.R. (1997), Regional Frequency Analysis an Approach Based on L-Moments, Cambridge University Press U.S.A.

Hussain, Z., and Pasha, G.R. (2008) Regional flood frequency analysis of the seven sites of Punjab, Pakistan, using L-moments.Water Resources Management 23.10 (2009): 1917-1933.

Hussain, Z. (2011) Application of the regional flood frequency analysis to the upper and lower basins of the Indus river, Pakistan. Water Resources Management 25(2011): 2797-2822.

Murat, A., and Ozgur, K. (2014).Investigation of trend analysis of monthly total precipitation by an innovative method.Theoretical and Applied Climatology 120: 617-629.

Malekinezhad, H., &Zare-Garizi, A. (2014).Regional frequency analysis of daily rainfall extremes using L-moments approach. Atmósfera, 27(4): 411- 427.

Rahman, M., Sarkar, S., Najati R., and Rai, R.K. (2013) Regional extreme rainfall mapping for Bangladesh using L-moment technique.Journal of Hydrologic Engineering. 2013.18:603-615.

Trefry, C.M., Watkins, D.W., and Johnson, D. (2005) Regional rainfall frequency analysis for the State of Michigan.Journal of Hydrologic Engineering 10(2005):437-449.

Wong, M., and Tung, Y-K.(2013) Regional frequency analysis of extreme rainfalls in Hong Kong.World Environmental and Water Resources Congress 2013 pp: 3276-3285.

Prediction Of Meteorological Drought In Western Rajasthan By Using SPI And MEI Indices

A.U.Chavadekar[1], S. S. Kashid[2]
[1]Research scholar, Walchand Institute of Technology, Solapur-413005,India.
[2]Professor at Walchand Institute of Technology, Solapur-413005. India
Email: ajaychavadekar@gmail.com , sskashid@yahoo.com
Telephone/Mobile No.: +919970794469, +919011579656

ABSTRACT

Drought is a deficit of water. Droughts are perceived as some of the most expensive and the least understood of natural disasters. Based on deficits observed in various hydrologic quantities, droughts are interpreted differently. For example, meteorological droughts are based on deficits in precipitation, agricultural droughts on deficits in soil moisture, and hydrologic droughts on stream flow deficits.

Drought modeling is normally done using the Standardized Precipitation Index (SPI).The SPI is a normal quintile transformation applied to a fitted parametric distribution of precipitation time series (McKee et al., 1993) Various drought prediction models have been developed by different researchers (Rao and Padmanabhan (1984), Loaiciga and Leipnik (1996) ,Lohani and Loganathan (1997), Kim and Valdés (2003)) . Climate systems are the most complex systems in nature for modeling. However the difficulties in modeling complex climate system are now considerably reduced by the recent 'Artificial Intelligence' tools like Artificial Neural Networks (ANNs); Genetic Algorithm (GA), Genetic Programming (GP) etc. Hence, this research work deals with development of models for prediction of droughts for frequently drought affected region of India i.e. Western Rajasthan. The predictions are based on Large-scale oceanic and atmospheric inputs viz. El Nino Southern Oscillation Index, Equatorial Indian Oscillation and Multivariate ENSO Index (MEI), using AI tool Genetic Programming. In this paper SPI index is predicted by using the predicted rainfall values.

Better correlation coefficient between observed and predicted rainfall were observed for combination of predictors viz. ENSO Index and EQUINOO Index. The correlation coefficients between observed rainfall and predicted rainfall were found to be remarkable. The drought events indicated by SPI-12 using GP predicted rainfall values were found to match with those Observed drought events indicated by SPI-12 index.

Keywords: Standardized Precipitation Index (SPI), EL Nino-Southern Oscillation (ENSO), Equatorial Indian Ocean Oscillation (EQUINOO), Multivariate ENSO Index (MEI), Genetic Programming (GP),

1. Introduction

Drought is a deficit of water. Droughts are perceived as some of the most expensive and the least understood of natural disasters. Based on deficits observed in various hydrologic quantities, droughts are

interpreted differently. Scarce rainfall in monsoon leads to drought situations. Shortage of food and fodder leads to massive devastating effect on human and animal. For mitigation of this affects government can plan, if it receives good forecast of drought before onset of monsoon.

Drought modeling is done using the Standardized Precipitation Index (SPI). SPI is simple to calculate, powerful and flexible index. In computation of SPI index only rainfall data is required as data input. By means of SPI indices we can identify dry periods and wet periods effectively. Drought is a temporary condition resulting from prolonged absence, deficiency, or poor distribution of precipitation (Ogallo, 1994; Wilhite, 1993). Although precipitation is the main controlling factor in drought events in the central Great Plains region (Wang, 2000), vegetation growth is dependent upon a number of additional environmental factors, such as high temperature, high winds, low soil moisture content, or low relative humidity. In particular, hydrologic soil properties play an important role in affecting vegetation growth (Sly, 1984; Farrar, Nicholson, & Lare, 1994; Nicholson & Farrar, 1994; Timlin, Loechel, Pachepsky, & Walthal, 2001). The total amount of water available for plant growth in a field is a function of the depth and water holding capacity of the soil, water holding capacity is considered one of the most influential hydrologic soil variables in calculating the amount of water storage in a soil profile (Brady & Weil, 2002; De Jong et al., 1984; Timlin et al., 2001; Wright, Boyer, Winant, & Perry, 1990). Figure 1 depicts the drought characteristics based on Standardized Precipitation Index (SPI). Shaded regions show drought events. The symbols ti and te show initiation and termination of the drought events.

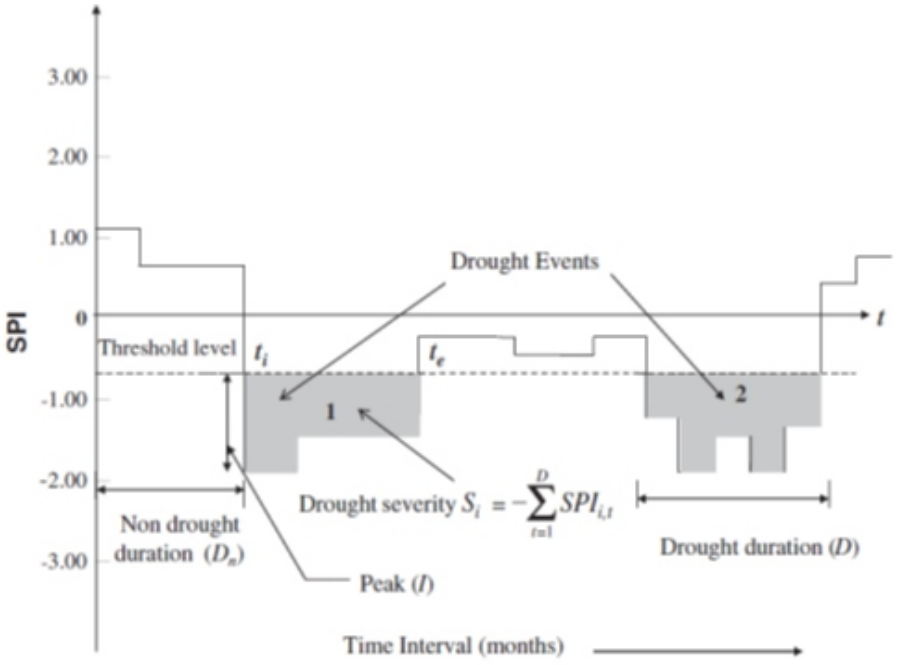

Figure 1: Depiction of drought characteristics (Severity, S; Duration, D; and peak I) based on Standardized Precipitation Index (SPI).

(Source: Poulomi Ganguli and M. Janga Reddy, 2013)

Simultaneous variations of climatic conditions and hydrologic variables over widely separated regions on the surface of earth have long been discovered and noted by the meteorologists, world over. Such recurrent patterns are commonly referred to as "hydroclimatic teleconnection". It is established that the natural variation of hydrologic variables is linked with these large-scale atmospheric circulation pattern through hydroclimatic teleconnection (Dracup and Kahya, 1994; Eltahir, 1996; Jain and Lall, 2001; Douglas et al., 2001; Ashok et al., 2001, 2004; Marcella and Eltahir, 2008; Maity and Nagesh Kumar, 2008). Indian hydrometeorology is prominently influenced by two large-scale atmospheric circulation patterns. The first is El Niño-Southern Oscillation (ENSO) from tropical Pacific Ocean and second is the Equatorial Indian Ocean Oscillation (EQUINOO) from Indian Ocean (Gadgil et al., 2004). El Niño-Southern Oscillation (ENSO), which is a large-scale circulation pattern from tropical Pacific Ocean, is established to influence Indian Summer Monsoon Rainfall and the droughts over Indian subcontinents. Another large scale circulation pattern from Indian Ocean viz. Indian Ocean Dipole Mode (IOD) also influences the Indian Summer Monsoon rainfall and droughts due to deficit rainfall (Saji et al., 1999). Equatorial Indian Ocean Oscillation (EQUINOO) is the atmospheric component of the IOD mode (Gadgil et al., 2003, 2004). Gadgil et al. (2003) have shown that the Indian Summer Monsoon Rainfall is not only associated with ENSO, but also with EQUINOO. They suggest that one can scientifically predict the Indian Summer Monsoon Rainfall by knowing the prior EQUINOO status. Equatorial zonal wind index (EQWIN) is considered as an index of EQUINOO, which is defined as negative of the anomaly of the zonal component of surface wind in the equatorial Indian Ocean Region. Since nearly 80% of Indian Summer Monsoon Rainfall is due to the southwest monsoon, interaction between various oceans due to ENSO and EQUINOO regulates the amount and distribution of the rainfall over the sub continent. Such association is more prominent for the large aerial scale. It is also prominent for longer temporal scale (seasonal) or smaller temporal scale (monthly).

Drought indices are typically designed for assessing current conditions and have little predictive capability. Hence, Large-scale oceanic and atmospheric indicators such as the El Nino-Southern oscillation phases, North Atlantic oscillations, Pacific North American index, Atlantic multidecadal oscillations, and Pacific decadal oscillations are used as long-term precursors to annual/seasonal forecasts of precipitation [Ropelewski and Halpert, 1996; McHugh and Rogers, 2001; Maity and Nagesh Kumar, 2008a].

The climate teleconnections with meteorological droughts were analysed and used to develop ensemble drought prediction models using a support vector machine (SVM)–copula approach over Western Rajasthan (India) by P. Ganguli and M. J. Reddy (2013). The meteorological droughts were identified using the Standardized Precipitation Index (SPI). They discussed about evaluation of trends and

multivariate frequency analysis of droughts in three meteorological subdivisions of western India.

1.1 Prediction of drought by predicting rainfall using ENSO, EQUINOO, MEI

1.1.1 El Niño-Southern Oscillation (ENSO)

El Niño-Southern Oscillation is a global coupled ocean-atmosphere phenomenon. The Pacific Ocean signatures, El Niño and La Niña are important temperature fluctuations in surface waters of the tropical Eastern Pacific Ocean. A higher El Ni˜no southern oscillation (ENSO) is associated with droughts and La Ni˜na is associated with of excess rainfall (Sikka 1980; Rasmusson and Carpenter 1983). For Indian subcontinent, the general impact of El Niño event is shown to be lower-than-normal rainfall, and the opposite in case of La Niña. (Rasmusson and Carpenter 1983; Khandekar and Neralla 1984; Ropelewski and Halpert 1987). It is found that summer monsoon rainfall over India is maximum correlated with SST from Niño 3.4 region.

1.1.2 Equatorial Indian Ocean Oscillation (EQUINOO)

Equatorial Indian Ocean Oscillation (EQUINOO) can be seen as the atmospheric component of the India Ocean Dipole (IOD) mode (Gadgil et al., 2003; 2004). During summer monsoon session (June-September), the convection over the eastern part of the equatorial Indian Ocean (90° E - 110° E, 10 ° S – 0 °) is negatively correlated to that over the western part of the equatorial Indian Ocean (50° E - 70° E, 10° S – 10° N). The anomalies in the sea level pressure and the zonal component of the surface wind along the equator are consistent with the convection anomalies. When the convection is enhanced (suppressed) over the western part of the equatorial Indian Ocean, anomalous surface pressure gradient high to low is towards the west (east) so that the anomalous surface wind along the equator becomes easterly (westerly). The oscillation between these two states is called the equatorial Indian Ocean Oscillation (EQUINOO) (Gadgil et al., 2003; 2004).

Equatorial zonal wind index (EQWIN) is considered as an index of EQUINOO, which is defined as negative of the anomaly of the zonal component of surface wind in the equatorial Indian Ocean Region (60o E - 90o E, 2.5 o S 2.5 o N).

1.1.3 Multivariate ENSO Index (MEI)

El Niño/Southern Oscillation (ENSO) is the most important coupled ocean-atmosphere phenomenon to cause global climate variability on interannual time scales. ENSO is monitored by basing the Multivariate ENSO Index (MEI) on the six main observed variables over the tropical Pacific. These six variables are: sea-level pressure (P), zonal (U) and meridional (V) components of the surface wind, sea

surface temperature (S), surface air temperature (A), and total cloudiness fraction of the sky (C). These observations have been collected and published in ICOADS for many years. The MEI is computed separately for each of twelve sliding bi-monthly seasons (Dec/Jan, Jan/Feb,..., Nov/Dec). After spatially filtering the individual fields into clusters (Wolter, 1987), the MEI is calculated as the first unrotated Principal Component (PC) of all six observed fields combined. This is accomplished by normalizing the total variance of each field first, and then performing the extraction of the first PC on the co-variance matrix of the combined fields (Wolter and Timlin, 1993). In order to keep the MEI comparable, all seasonal values are standardized with respect to each season and to the 1950-93 reference periods.

2.0 Objectives of the work

This work intends to develop monthly rainfall prediction models for medium range (1 month ahead) forecasts of monthly Indian Summer Monsoon rainfall leading to drought prediction (if any) for 'Western Rajasthan' sub division of India, by using ENSO, EQUINOO and MEI indices as large scale atmospheric circulation information, with the help of Artificial Intelligence tool Genetic Programming.

3.0 Data

Monthly rainfall data over all sub divisions of India (http://www.tropmet.res) (Parthasarathy et al. 1995) used for this study were collected by India Meteorological Department for a period 1871–2010. The data from 1950 through 2010 were only used, as the ENSO and EQUINOO data were available 1950 onwards. Monthly rainfall data from data from 1950 through 1975 were used for the Training purpose. The data from 1976 through 1990 were used for the validation purpose. The data from 1991 through 2010 were used as testing the GP models. The analysis consists of rainfall depths all over India for so called Indian Summer Monsoon season (June to September) plus the month of October.

Sea surface temperature (SST) anomaly from the Niño 3.4 region (120^{o} W–170^{o} W, 5^{o} S–5^{o} N) is used as the 'ENSO index' in this study. Monthly sea surface temperature data from Niño 3.4 region for the period, January 1950 to December 2010, data are obtained from the website of the National Weather Service, Climate Prediction Centre of National Oceanic and Atmospheric Administration (NOAA) (http://www.cpc.noaa.gov/data/indices/ and http://www.cpc.ncep.noaa.gov).

EQWIN, the negative of zonal wind anomaly over equatorial Indian Ocean region (60^{o}E – 90^{o} E, 2.5S - 2.5N) is used as 'EQUINOO index' (Gadgil et al., 2004). Monthly surface wind data for the period January 1950 - December 2010, are obtained from the National Centre for Environmental Prediction (http://www.cdc.noaa.gov/Datasets).

MEI is re-computed every month to monitor the strength of ENSO conditions for the preceding two months. The discussion of the MEI time-series and spatial patterns can be seen on (http://www .cdc.noaa.god-kewlMEI/). It is updated during the first week of each following month.

The MEI is computed separately for each of twelve sliding bi-monthly seasons (Dec/Jan, Jan/Feb,..., Nov/Dec). After spatially filtering the individual fields into clusters (Wolter, 1987), the MEI is calculated as the first unrotated Principal Component (PC) of all six observed fields combined. This is accomplished by normalizing the total variance of each field first, and then performing the extraction of the first PC on the co-variance matrix of the combined fields (Wolter and Timlin, 1993). In order to keep the MEI comparable, all seasonal values are standardized with respect to each season and to the 1950-93 reference period.

4.0 Methodology

Methodology is broadly divided in 4 steps

- Data collection from source and data management for prediction of rainfall.
- Prediction of rainfall with given inputs by using Genetic Programming.
- Computation of SPI-12 index for observed and predicted rainfall.
- Identification of drought and prediction of drought intensity by using SPI-12 index.

Data are collected from above mentioned sources and data management is done by using the software MS Excel. Input files for prediction of rainfall are created by arranging the rainfall data and predictors. Prediction of rainfall is done by using the Artificial Intelligence tool Genetic Programming.

Genetic Programming is widely used in recent years for data mining, rainfall runoff modeling and other hydrologic predictions (Babovic, 2005; Babovic and Keijzer, 2002; Liong et al., 2002). Prediction of meteorological events such as rainfall over a region is much more complex task due to extreme instability of the atmosphere. Such complex systems can be considerably reduced by using the modern Artificial Intelligence (AI) tools like Artificial Neural Networks (ANNs), Genetic Algorithm (GA) and Genetic Programming (GP). GP is an evolutionary computing family, so it creates a lot of computer programs. (Sette and Boullart, 2001;Saks and Maringer, 2010). GA usually operates on (coded) strings of numbers, whereas GP operates on computer programs. Genetic Programming can solve much more complicated problems. Genetic Programming can also be applied to a greater diversity of problems (Koza, 1992).

The influence of ENSO and EQUINOO on regional Indian Summer Monsoon Rainfall varies from

region to region. The highest correlation between observed rainfall and predicted rainfall is observed for Central North-East India and West Central India followed by North East and North West regions of India. The GP based method proposed in this research is demonstrated in the contest of Indian Summer Monsoon rainfall prediction which is dependent on ENSO and EQUINOO indices.(S.S. Kashid and Rajib Maity(2012))

4.1 Genetic Programming

Genetic Programming breeds a population of computer programs to solve a problem. (Koza, 1992). Five major preparatory steps in application of GP (Koza, 1992) can be summarized as following:

(I) selection of the set of terminals,

(ii) selection of the set of primitive functions,

(iii) deciding the fitness measure,

(iv) deciding the parameters for controlling the run, and

(v) defining the method for designating a results and the criterion for terminating a run.

The choice of input variables is generally based on prior knowledge of casual variables and physical insight into the problem being studied. If the relationship to be modeled is not well understood, then analytical techniques can be used. GP evolves a function that relates the input information to the output information, which is of the form:

$$Y^m = f(X^n) \quad (1)$$

Where X^n is an n-dimensional input vector and Y^m is an m-dimensional output vector.

GP has the unique feature that it does not assume any functional form of the solution. GP can optimize both the structure of the model and its parameters. Genetic Programming evolves a computer program, relating the output and input variables. The specialty of GP approach lies with its ability to select input variables that contribute beneficially to the model and to disregard those that do not. Hence Genetic Programming is used for modeling regional rainfall prediction in this study.

In the proposed study, the input vector consists of Historical Average Rainfall for particular month, ENSO, EQUINOO and MEI indices of three previous monthly time steps. The output vector consists of monthly rainfall for the particular month over the region.

In this work GP is implemented through Discipulus (Francone, 1998) software that is based on an extension of the originally envisaged GP called Linear Genetic Programming (LGP). Genetic programs normally represent highly non-linear solutions (Brameier and Banzhaf, 2004).

4.1.1 Control parameters and input impact of different variables

Initially Values of control parameters of Genetic Programming can be selected and varied in trials till the best fitness measures are produced. The fitness criterion is the mean squared error between the actual and the predicted values. The statistical error criteria of Correlation Coefficient (C.C.) between observed and predicted rainfall and Root Mean Square Error (RMSE) have been used in this study to compare the GP predictions with the actual observations.

Four basic arithmetic operators (+, _, *, /), trigonometric functions and some basic mathematical functions like sqrt (x) and power are utilized. In this study GP control parameters adopted are as follows: Population size: 500, number of generations: 300, mutation frequency: 90%, crossover frequency: 50%. The reproduction rate in a run is left over after the application of the crossover and mutation operators. The reproduction rate may be calculated (in percentage) as follows:

Reproduction rate = 100 - mutation rate - (crossover rate * [1 -mutation rate])

Main inputs in this study are monthly values of ENSO indices, EQUINOO indices and MEI indices of few previous months. The values are taken for three previous monthly time steps. This it was decided to use ENSO, EQUINOO and MEI indices of time steps (t - 1), (t - 2) and (t - 3) with climatological mean rainfall of the particular month, as inputs. This combination could give the best results.

4.1.2 Genetic programming approach for monthly rainfall forecasting

Monthly rainfall data, ENSO, EQUINOO and MEI indices from, 1950 to 2010 was used for this study. ENSO, MEI and EQUINOO indices for three immediate previous months are considered for monthly rainfall prediction.

4.2 Monthly Rainfall Prediction of Western Rajasthan

The analysis in this study carried out, uses the large-scale atmospheric circulation pattern ENSO, EQUINOO and MEI indices of three previous time steps for prediction of monthly rainfall. This can be treated as medium range forecast with one month lead time, which has its own importance for planning of agricultural activities and judicious management of available water in reservoirs.

Here we have tried four different combinations of predictors as:

(1) MEI

(2) ENSO + EQUINOO

(3) MEI + EQUINOO

Thus the monthly rainfall is modeled as a function of

(i) Historical average monthly rainfall of the particular month (HRt),

(ii) ENSO indices of three previous monthly time steps (EN),

(iii) MEI indices of three previous monthly time steps (MEI),

(iv) EQUINOO indices of three previous monthly time steps (EQ).

The pairs of equations for the aforesaid four combinations are listed as following:

$$R_t = f\{(HR_t),\ (MEI_{t-3},\ MEI_{t-2},\ MEI_{t-1})\} \quad \ldots\ldots(1)$$
$$R_{Jun} = f\{(HR_{Jun}),\ (MEI_{March},\ MEI_{April},\ MEI_{May})\} \quad \ldots\ldots(2)$$

$$R_t = f\{(HR_t),\ (EN_{t-3},\ EN_{t-2},\ EN_{t-1})(EQ_{t-3},\ EQ_{t-2},\ EQ_{t-1})\} \quad \ldots\ldots(3)$$
$$R_{Jun} = f\{(HR_{Jun}),(Un_{mark},\ EN_{April},\ EN_{May})(EQ_{March},\ EQ_{April},\ EQ_{May})\} \quad \ldots\ldots(4)$$

$$R_t = f\{(HR_t),(MEI_{t-3},\ MEI_{t-2},\ MEI_{t-1}),(EQ_{t-3},\ EQ_{t-2},\ EQ_{t-1})\} \quad \ldots\ldots(5)$$
$$R_{June} = f\{(HR_{June}),(MEI_{March},\ MEI_{April},\ MEI_{May}),(EQ_{March},\ EQ_{April},\ EQ_{May})\} \quad \ldots\ldots(6)$$

Thus the total summer monsoon rainfall is sum of rainfall from June through September, calculated as following.

$$R_{monsoon} = R_{June} + R_{July} + R_{August} + R_{September} \quad \ldots\ldots(7)$$

Where Rt stands for predicted rainfall of particular month, HR stands for Historical average of rainfall in particular month, EN stands for ENSO index, EQ stands for EQUINOO Index, MEI stands for multivariate ENSO index. The optimum number of lags to be considered for each input variables was is decided based on the 'input impacts' of that input variable during model calibration.

4.3 Computational Methodology of SPI Index

The SPI is a normal quantile transformation applied to a fitted parametric distribution of precipitation time series (McKee et al., 1993). This SPI can characterize drought at multiple timescales such as 3, 6, 9 or 12 months to capture different drought states ranging from short-term, medium-term and long-term drought conditions. In this study, SPI at a 12-month timescale (SPI-12) is chosen for drought modeling, which can be useful for assessing seasonal drought conditions. The details of computation of the SPI can be found in McKee et al. (1993) and Janga Reddy and Ganguli (2012). A drought period is identified when the SPI value falls below a threshold level, which is taken as the 20thpercentile value (Svoboda et al., 2002). Figure 1 illustrates drought characteristic identification using SPI. Drought length or duration (D) is taken as the number of consecutive time intervals (months) where SPI remains below the threshold level. Drought severity (S) is the cumulative values of SPI within the drought duration.

For convenience, the severity of drought event I, is taken as positive and given as $S_i = -\sum_{t=1}^{D} SPI_{i,t}$

Table 1: Classification of Droughts According to SPI Index

SPI Index	Drought Intensity Designation
2.0+	Extremely wet
1.5 to1.99	Very Wet
1.0 to1.49	Moderately wet
-0.99 to 0.99	Near Normal
-1.0 to -1.49	Moderately dry
-1.5 to -1.99	Severely dry
-2 to less	Extremely dry

5.0 Results and Discussions

The analysis performed here can be treated as a real time analysis, which uses large scale atmospheric circulation pattern indices of three previous months to predict rainfall of current month. The methodology is discussed as following.

5.1 Rainfall Analysis Using ENSO, EQUINOO and MEI

Presently detailed study and drought identification of western Rajasthan is completed. Western Rajasthan with an area of 196,150 Km2 occupies 57.31% of India's total arid zone area. The climate is characterized by low, highly variable and ill-distributed rainfall, high wind speed, high evaporation losses, and extremes of seasonal temperatures. Rajasthan has only 1% of the country's total surface water resources. The monsoon period is short about 2 to 3 months (July-September), resulting in annual rainfall ranging from 150-900 mm in different part of the state (average annual precipitation 576 mm) and temperature varies from 5ºC-45ºC in different seasons (RACP 2012). Rainfall analysis using MEI, ENSO and EQUINOO Long term average (1950–2010) computed. Monthly average Rainfall (mm) values of during monsoon months June to September is given in Table 2.

Table 2 Average Monthly Rainfall (mm) for Western Rajasthan during Monsoon Months June through September

No	Region	June (mm)	July (mm)	August(mm)	September (mm)	Total monsoon (Jun–Sept) (mm)
1	Western Rajasthan	34.44	94.73	93.94	41.52	264.63

As only June through September rainfall is treated as 'monsoon rainfall by India Meteorological Department, June through September rainfall values are summed while reporting 'monsoon rainfall' in

this work. Monthly rainfall values during months June through October have been computed by Genetic Programming models. Monthly rainfall anomalies of observed and computed rainfall with reference to long term average (1950–2010) are also computed and presented through plots. The monthly rainfall values over Training period, validation period and Testing period for All India Summer Monsoon Rainfall can be visualized through charts.

Graphical Presentation of Observed and Predicted of all India with (ENSO+EQUINOO) combination during training and testing is shown in Fig. 3(a) and Fig. 3(b) respectively.

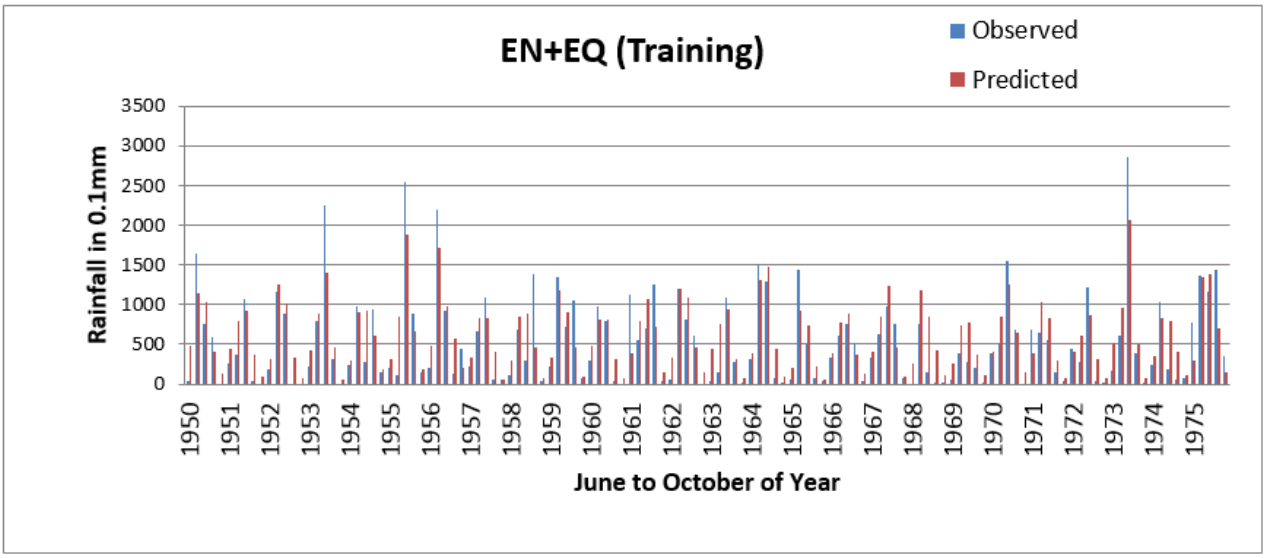

Figure 3 (a) Graphical Presentation of Observed and Predicted of all India with (EN+EQ) combination (Training)

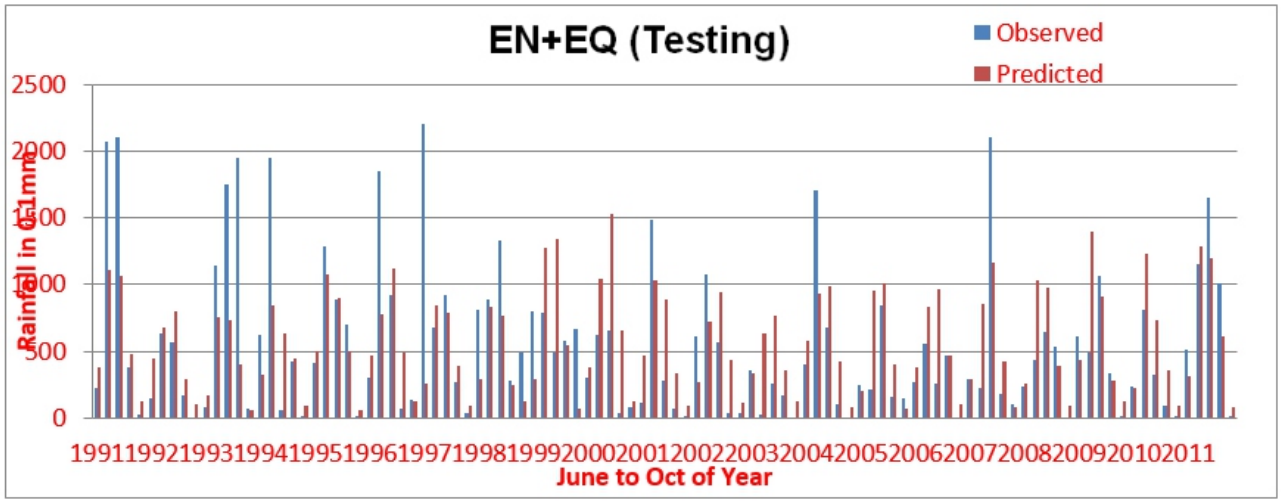

Figure 3 (b) Graphical Presentation of Observed and Predicted of all India with (EN+EQ) combination (Testing)

The joint influence of ENSO and EQUINOO is established in earlier studies (Gadgil et al., 2004; Maity

and Nagesh Kumar, 2006). Three monthly time lags of ENSO, EQUINOO and MEI are considered in this analysis. The earlier study by Maity and Nagesh Kumar (2006) uses two monthly lags for ENSO and one monthly lag for EQUINOO. However the reason behind using three monthly lags in this analysis, which is nothing but medium range forecast with 2 weeks lead time. It is interesting to see that the highest Correlation Coefficient in Testing of GP model for 3 combination as [EN+EQ],[MEI],[MEI+EQ] for monthly rainfall has been observed for 'All India Rainfall', treating India as a single unit.

Rainfall is predicted by three combinations of the climatic predictors. The combination are tried to achieve better and better predictions. The various combinations of input variables tried to predict rainfall are (1) EQ+MEI, (2) MEI (3) EQ+ENSO. Therefore, rainfall predicted three times by three combinations. SPI-12 index is calculated two times for each combination for observed and predicted rain fall.

Best correlations between observed and predicted rainfall were achieved for [ENSO+EQUINOO] significant difference in C.C. over Western Rajasthan region. The Pearson product moment Correlation Coefficients for Training, and Testing for Western Rajasthan regions are tabulated in Table 3. Root Mean Square Error For measurement of rainfall in mm during Training and Testing are enlisted in Table 4.

Table 3: Correlation Coefficients between observed and predicted rainfall during Training and Testing

Regions	CC	EN+EQ	MEI	MEI+EQ
Western Rajasthan	Training	0.85	0.86	0.834
	Testing	0.552	0.55	0.495

Table 4: Root Mean Square Error For measurement of rainfall in mm during Training and Testing

Regions	RMSE	EN+EQ	MEI	MEI+EQ
Western Rajasthan	Training	32.02	29.5	30.477
	Testing	44.17	45.64	47.03

For first combination of predictor (ENSO and EQUINOO) Person Co-relation coefficient for observed and predicted rainfall is 0.850 and 0.496 respectively. Drought identification is carried out by calculating SPI-12 index for both observed and predicted rainfall. From SPI-12 values it is observed that 4 severely dry events identified in year 1951-53, 70-71,85-86,2002-03 and 6 moderately dry events identified for observed rainfall. At the same time for predicted rainfall 3 Severely dry events identified out of that two severe droughts events and their duration perfectly matching with observed drought, Similarly moderately dry events and duration also matching with observed droughts.

From Figure 4 it is observed that observed droughts events are nearly matching with predicted drought events. By these studies we can give early warnings of droughts.

Table 5. Observed and Predicted Droughts by Rainfall Prediction EN+EQ

SPI-12 by Observed Rainfall			SPI-12 by Predicted Rainfall (EN+EQ)		
Drought Year	Duration (Months)	Type	Drought Year	Duration (Months)	Type
1951-53	24	Severely dry	1951-52	22	Moderately dry
1957-58	12	Moderately dry	1957-58	11	Moderately dry
			1968-69	12	Moderately dry
1970-71	12	Severely dry	1969-71	23	Severely dry
1974-75	10	Moderately dry			
1985-86	12	Severely dry	1985	3	Moderately dry
1987-88	5	Moderately dry	1987	2	Moderately dry
1989	3	Moderately dry			
1992-93	9	Moderately dry	1992-93	3	Moderately dry
			1994-95	8	Moderately dry
			1997-98	12	Severely dry
2002-03	11	Severely dry	2002-03	11	Severely dry
2009-10	9	Moderately dry			

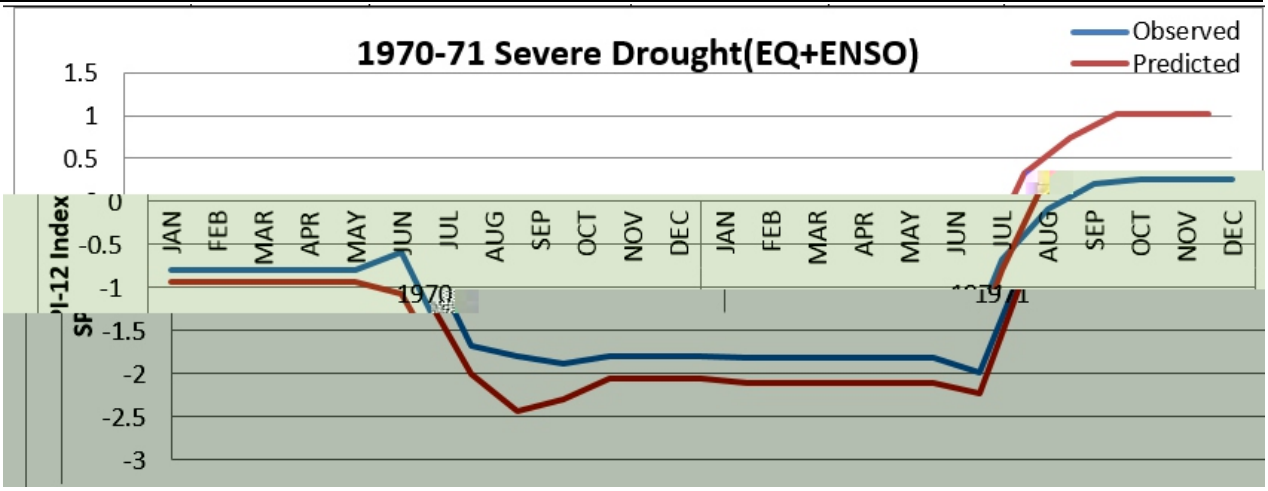

Figure 4 Severe Observed and Predicted Historic Drought event Western Rajasthan

In second combination (MEI) index is taken as predictor and rainfall is predicted. Droughts identified by SPI-12 for this combination given below Table No.6 Total 8 drought events identified out of these 3 droughts are severe and 5 droughts are moderate. It seems that most of drought events are matching with observed droughts but its intensity is fluctuating and classification is changing.

Table 6. Observed and Predicted Droughts by Rainfall Prediction using MEI

SPI-12 by Observed Rainfall			SPI-12 by Predicted Rainfall (MEI)		
Drought Year	Duration (Months)	Type	Drought Year	Duration (Months)	Type
1951-53	24	Severely dry	1951	6	Moderately dry
1957-58	12	Moderately dry	1957-58	2	Moderately dry
			1969	2	Moderately dry
1970-71	12	Severely dry			
1974-75	10	Moderately dry			
1985-86	12	Severely dry			
1987-88	5	Moderately dry	1987-88	14	Severely dry
1989	3	Moderately dry			
1992-93	9	Moderately dry	1992-93	11	Severely dry
			1994-95	8	Moderately dry
			1997-98	13	Severely dry
2002-03	11	Severely dry	2002-03	11	Moderately dry
2009-10	9	Moderately dry			

In third combination of predictor EQUINOO and MEI is use as predictor. Total 9 drought events are identified out of that 2 are severe and remaining are moderate. Again in this combination there is close association between observed and predicted SPI-12 Results but intensity reducing.

Table 7. Observed and Predicted Droughts by Rainfall Prediction EQUINOO and MEI

SPI-12 by Observed Rainfall			SPI-12 by Predicted Rainfall (EQ+MEI)		
Drought Year	Duration (Months)	Type	Drought Year	Duration (Months)	Type
1951-53	24	Severely dry			
1957-58	12	Moderately dry			
			1965-66	16	Moderately dry
1970-71	12	Severely dry	1969-70	10	Moderately dry
			1972-73	11	Moderately dry
1974-75	10	Moderately dry			
			1982-83	12	Severely dry
1985-86	12	Severely dry	1986	2	Moderately dry
1987-88	5	Moderately dry	1987-88	11	Severely dry
1989	3	Moderately dry			
1992-93	9	Moderately dry	1992-94	21	Moderately dry
			1998-99	11	Moderately dry
2002-03	11	Severely dry	2003-04	10	Moderately dry
2009-10	9	Moderately dry			

5.0 Conclusions

This work uses the association between the large-scale circulation patterns for prediction of Indian Summer Monsoon Rainfall and drought over Western Rajasthan regions of India which is quite important for drought mitigations. Genetic programming approach is used for establishing the complex relationship between inputs and outputs. Various combinations of predictors viz. ENSO, EQUINOO and MEI were explored for the monthly rainfall prediction. Historical average rainfall of the particular month was invariably used in each of the Combinations. Highest correlation was observed in combination of ENSO and EQUINOO. However, combination of ENSO and EQUINOO is found better compared to other predictor combinations and drought events predicted by this combination with SPI-12 indices are nearly matching with observed events.

6.0 References

1. Aytek, A., Kisi, O., 2008. A genetic programming approach to suspended sediment modeling. J. Hydrol. 351, 288–298.

2. Banerjee, A. K., Sen, P. N., Raman, C. R. V., 1978. On foreshadowing southwest monsoon rainfall over India with mid-tropospheric circulation anomaly of April. Indian J. Meteorol. Hydrol. Geophys. 29, pp.425–431.

3. Babovic, V., Keijzer, M., 2000. Genetic programming as a model induction engine. J. Hydroinform. 2 (1), 35–60.

4. Bhalme, H. N., Jadhav, S. K., Mooley, D. A., Ramana Murty, B. H. V., 1986. Forecasting of monsoon performance over India. J. Climatol., 6, pp. 347–354.

5. Boschat G, Pascal Terray and Sebastien Masson 2012 Robustness of SST teleconnections and precursory patterns associated with the Indian summer monsoon; Clim. Dynam. 38 2143–2165

6. D'Arrigo R, Smerdon JE. 2008. Tropical climate influences on drought variability over Java, Indonesia. Geophysical Research Letters 35: L05707. DOI: 10.1029/2007GL032589.

7. Gadgil, S., P. N. Vinayachandran, P. A. Francis, and S. Gadgil (2004), Extremes of the Indian Summer monsoon rainfall, ENSO and equatorial Indian Ocean Oscillation, Geophys. Res. Lett., 31, L12213,.

8. Gowariker, V., Thapliyal, V., Kulshrestha, S.M., Mandal, G.S., Sen Roy, N., Sikka, D.R.,1991. A power regression models for long range forecast of southwest monsoon rainfall over India. Masaum 42, 125–130.

9. Identification of hydrologic drought triggers from hydroclimatic predictor variablesRajib Maity,1 Meenu Ramadas,2 and Rao S. Govindaraju2WATER RESOURCES RESEARCH, VOL. 49, 4476–4492, doi:10.1002/wrcr.20346, 2013

10. Janga Reddy M, Ganguli P. 2012. Application of copulas for derivation of drought severity-duration-frequency curves. Hydrological Processes 26(11): 1672–1685.

11. Kashid and Maity (2012), Prediction of monthly rainfall on homogeneous monsoon regions of India based on large scale circulation patterns using Genetic Programming, Elsevier, Journal of Hydrology 454–455, pp. 26–41.

12. Kashid and Maity (2009), Kashid and Maity (2009), Short-Term Basin-Scale Streamflow Forecasting Using Large-Scale Coupled, Atmospheric–Oceanic Circulation and Local Outgoing Longwave Radiation, Elsevier, Journal of Hydrology DOI: 10.1175/2009JHM1171.1

13. Li, X.Y., Chau, K.W., Cheng, C.T., Li, Y.S., 2006. A Web-based flood forecasting system for Shuangpai region. Adv. Eng. Softw. 37 (3), 146–158.

14. McKee, T. B., N. J. Doesken, and J. Kleist, 1993: The relationship of drought frequency and duration of time scales. Eighth Conference on Applied Climatology, American Meteorological Society, Jan17-23, 1993, Anaheim CA, pp.179-186.

15. Muttil, N., Chau, K.W., 2007. Machine learning paradigms for selecting ecologically significant input variables. Eng. Appl. Artif. Intell. 20 (6), 735–744.

16. Partal, T., Kisi, O., 2007. Wavelet and neuro fuzzy conjunction model for precipitation forecasting. J. Hydrol. 342, 199–212.

17. P. GANGULI AND M. J Genest C, Rémillard B, Beaudoin D. 2009. Goodness-of-fit tests forcopulas: a review and a power study. Insurance: Mathematics and Economics 44: 199–213.

18. Parthasarathy, B., H. F. Diaz, and J. K. Eischeid (1988), Prediction of all India summer monsoon rainfall with regional and large-scale parameters ,J. Geophys. Res., 93(5), 5341–5350,. Sci. 86(3), pp. 22–431.

19. Parthasarathy, B., Rupa Kumar, K., Deshpande, V.R., 1991. Indian summer monsoon rainfall and 200mb meridional wind index: application for long range prediction. Int. J. Climatol. 11, 165 176
20. .Parthasarathy, B., Munot, A.A., Kothawale, D.R., 1995. Monthly and Seasonal Rainfall Series for All-India Homogeneous Regions and Meteorological Subdivisions:1871–1994. IITM Research, Report No. RR-065.
21. Rajeevan, M., Pai, D.S., Dikshit, S.K., Kelkar, R.R., 2004. IMD's new operational models for long-range forecast of southwest monsoon rainfall over India and their verification for 2003. Curr. Sci. 86 (3), 22–431
22. Rajeevan M, Unnikrishnan C K and Preethi B 2012 Evaluation of the ENSEMBLES multi-model seasonal forecasts of Indian summer monsoon variability; Clim. Dynam. 38 2257–2274
23. Rasmusson E M and Carpenter T H 1983 The relationship between eastern equatorial Pacific sea surface temperatures and rainfall over India and Sri Lanka; Mon. Weather Rev. 111 517–528.
24. Rao, K.N., 1965. Seasonal forecasting – India. Proc. of Symp. on 'Research and Development Aspects of Long Range Forecasting'. WMO-IUGG Tech. Note No. 66 WMO-No. 162-TP-79. World Meteorological Organisation Geneva, pp. 17–30.
25. Rao, K.N., Rama Moorthy, K.S., 1960. Seasonal (Monsoon) rainfall forecasting in India. Proc. of Symp. on 'Monsoon of the World', held at New Delhi February 1958, Published by India Meteorological Department, New Delhi, pp. 237–250.
26. National Drought Mitigation Center, University of Nebraska-Lincoln, U.S.A.
27. Ropelewski, C. F., and M. S. Halpert (1987), Global and regional scale precipitation patterns associated with the El Nin˜o/Southern Oscillation,Mon. Weather Rev., 115, 1606– 1626.
28. Savur, S.R., 1931. The seasonal Forecasting Formulae Used in the India Meteorological Department. Scientific Notes, vol. 4, no. 37. Published by India Meteorological Department, New Delhi.
29. Sette, S., Boullart, L., 2001. Genetic programming: principles and applications. Eng.Appl. Artif. Intell. 14, 727–736
30. Sikka D R 1980 Some aspects of the large-scale fluctuations of summer monsoon rainfall over India in relation to fluctuations in the planetary and regional scale circulation parameters; Proc. Indian Acad. Sci. (Earth Planet. Sci.) 89 179–195
31. Shiri, J., Kisi, O., 2011. Application of artificial intelligence to estimate daily pan evaporation using available and estimated climatic data in the Khozestan Province (Southwestern Iran). ASCE J. Irrig. Drain. Eng. 137 (7), 412–425.
32. Shukla, J., Paolino, D.A., 1983. The Southern Oscillation and long range forecasting of the summer monsoon over India. Mon. Weather Rev. 111, 1830–1837.
33. Wolter, K., 1987: The Southern Oscillation in surface circulation and climate over the tropical Atlantic, Eastern Pacific, and Indian Oceans as captured by cluster analysis. J. Climate Appl. Meteor., 26, 540-558
34. Wolter, K., and M.S. Timlin, 1993: Monitoring ENSO in COADS with a seasonally adjusted principal component index. Proc. of the 17th Climate Diagnostics Workshop, Norman, OK, NOAA/NMC/CAC, NSSL, Oklahoma Clim. Survey, CIMMS and the School of Meteor., Univ. of Oklahoma, 52-57.

Prediction Of Monthly Rainfall On Homogeneous Monsoon Regions Of India Based On Large Scale Circulation Patterns Using Genetic Programming

Vaishalee S.Khotlande[1], **Satishkumar S. Kashid**[2]
[1]Research scholar, Walchand Institute of Technology, Solapur-413005,India.
[2]Professor at Walchand Institute of Technology, Solapur-413005. India
Email: vaishalikhotlande@gmail.com ,sskashid@yahoo.com

ABSTRACT

Indian Summer Monsoon Rainfall (ISMR) is found to vary annually leading to profound impact on agriculture. Hence monsoon forecast is always in great demand by government and farming community. The Large-scale atmospheric circulation patterns are proven to influence the Indian Summer Monsoon Rainfall. EL Nino-Southern Oscillation (ENSO) and Equatorial Indian Ocean Oscillation (EQUINOO) have shown major influence on ISMR. Recently 'Multivariate ENSO Index (MEI)' is also used to represent ENSO on basis of six main observed variables over the tropical Pacific. Hence ENSO, EQUINOO and MEI indices are used to develop models for prediction of monthly Indian summer monsoon rainfall. This work develops models for medium range forecasts, for five homogeneous monsoon regions of India. For developing these models, recent Artificial Intelligence tool- Genetic Programming has been used. The correlation coefficient between observed rainfall and predicted rainfall for different combination of predicators and regions are calculated.

It is observed that better correlation coefficient between observed rainfall and predicted rainfall were found to for [ENSO+EQUINOO] combination of predictors for most of the regions. The correlation coefficient between observed rainfall and predicted rainfall were found to be highest for All India predications due to large spatial extend of the area under consideration.

Keywords: EL Nino-Southern Oscillation (ENSO), Equatorial Indian Ocean Oscillation (EQUINOO), Multivariate ENSO Index (MEI), Genetic Programming (GP), Indian Summer Monsoon Rainfall (ISMR)

1. Introduction

Indian Summer Monsoon Rainfall (ISMR) is always found to vary annually, leading to profound impacts on agriculture based Indian economy. Spatiotemporal distribution of rainfall and amount of monsoon rainfall influences many policy decisions at National level. Prediction of Monsoon rainfall has been remained a great challenge for hydro-meteorologists due to inherent complexities in modeling the climatic systems

There is a strong link between the interannual variation of Indian summer monsoon rainfall (ISMR) and

El Ni˜no southern oscillation (ENSO).Equatorial Indian Ocean oscillation (EQUINOO) plays an important role. (Gadgil et al. 2003, 2004, 2007; Ihara et al. 2007; Francis and Gadgil 2010; Boschat et al. 2012; Rajeevan et al. 2012). Recent studies have shown that, in addition to El Ni˜no southern oscillation (ENSO) and equatorial Indian Ocean oscillation (EQUINOO), Multivariate ENSO Index (MEI) is also considered as the most representative index, since it links six different meteorological parameters measured over the tropical Pacific.

1.1 Prediction of ISMR using ENSO, EQUINOO and MEI

1.1.1 El Niño-Southern Oscillation (ENSO)

El Niño-Southern Oscillation is a global coupled ocean-atmosphere phenomenon. The Pacific Ocean signatures, El Niño and La Niña are important temperature fluctuations in surface waters of the tropical Eastern Pacific Ocean. A higher El Ni˜no southern oscillation (ENSO) is associated with droughts and La Ni˜na is associated with of excess rainfall (Sikka 1980; Rasmusson and Carpenter 1983).

The intensities of El Niño are generally assessed on the basis of the average SST over the different Niño regions in the Pacific Ocean, widely known as Niño 1(10° S - 5° S, 90° W - 80° W), Niño 2 (5° S - 0°, 90° W - 80° W), Niño 3 (5° S - 5° N, 90°W - 150 ° W), Niño 3.4 (5° S - 5 ° N, 170° E-120° W) and Niño 4 (5° S - 5 ° N, 160° E-150° W). A map of tropical Pacific Ocean showing the above region is shown in Figure 1.

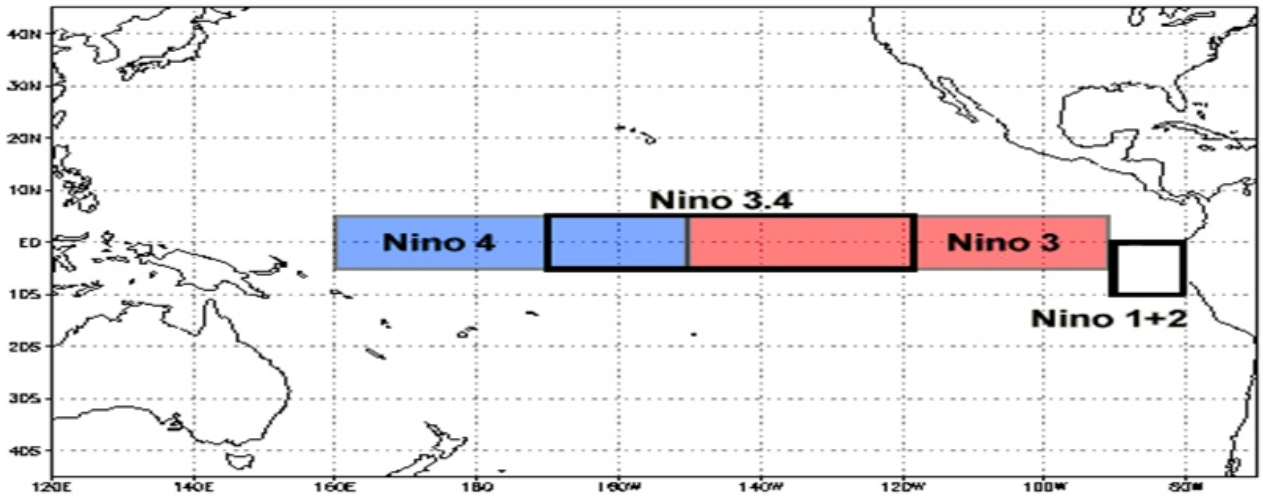

Figure 1 Locations of different Niño regions (Source: http://www.srh.noaa.gov)

1.1.2 Equatorial Indian Ocean Oscillation (EQUINOO)

Equatorial Indian Ocean Oscillation (EQUINOO) can be seen as the atmospheric component of the India Ocean Dipole (IOD) mode (Gadgil et al., 2003; 2004). During summer monsoon session (June

September), the convection over the eastern part of the equatorial Indian Ocean (90° E - 110°E, 10° S – 0 °) is negatively correlated to that over the western part of the equatorial Indian Ocean (50° E - 70° E, 10° S – 10° N). The anomalies in the sea level pressure and the zonal component of the surface wind along the equator are consistent with the convection anomalies. When the convection is enhanced (suppressed) over the western part of the equatorial Indian Ocean, anomalous surface pressure gradient high to low is towards the west (east) so that the anomalous surface wind along the equator becomes easterly (westerly). The oscillation between these two states is called the equatorial Indian Ocean Oscillation (EQUINOO) (Gadgil et al., 2003; 2004).

Equatorial zonal wind index (EQWIN) is considered as an index of EQUINOO, which is defined as negative of the anomaly of the zonal component of surface wind in the equatorial Indian Ocean Region (60° E - 90°E, 2.5 ° S 2.5 ° N).

1.1.3 Multivariate ENSO Index (MEI)

El Niño/Southern Oscillation (ENSO) is the most important coupled ocean-atmosphere phenomenon to cause global climate variability on interannual time scales. ENSO is monitored by basing the Multivariate ENSO Index (MEI) on the six main observed variables over the tropical Pacific. These six variables are: sea-level pressure (P), zonal (U) and meridional (V) components of the surface wind, sea surface temperature (S), surface air temperature (A), and total cloudiness fraction of the sky ©.

2.0 Objectives of the work

This work intends to develop models for medium range (1 month ahead) forecasts of monthly Indian Summer Monsoon rainfall for 'All India', as well as for five homogeneous monsoon regions of India, by using ENSO, EQUINOO and MEI indices as large scale atmospheric circulation information, with the help of Artificial Intelligence tool Genetic Programming.

3.0 Data

Sea surface temperature (SST) anomaly from the Niño 3.4 region (120° W–170° W, 5° S–5 ° N) is used as the 'ENSO index' in this study. Monthly sea surface temperature data from Niño 3.4 region for the period, January 1950 to December 2010, data are obtained from the website of the National Weather Service, Climate Prediction Centre of National Oceanic and Atmospheric Administration (NOAA) (http://www.cpc.noaa.gov/data/indices/ and http://www.cpc.ncep.noaa.gov).

EQWIN, the negative of zonal wind anomaly over equatorial Indian Ocean region (60°E – 90° E, 2.5S - 2.5N) is used as 'EQUINOO index' (Gadgil et al., 2004). Monthly surface wind data for the period

January 1950 - December 2010, are obtained from the National Centre for Environmental Prediction (http://www.cdc.noaa.gov/Datasets).

MEI is re-computed every month to monitor the strength of ENSO conditions for the preceding two months. The discussion of the MEI time-series and spatial patterns can be seen on (http://www.cdc.noaa.god-kewlMEI/). It is updated during the first week of each following month.

Monthly rainfall data over entire India as well as over homogeneous monsoon regions of India rainfall data (http://www.tropmet.res) (Parthasarathy et al. 1995) used for this study were collected by India Meteorological Department for a period 1871–2010. The data from 1950 through 2010 were only used, as the ENSO and EQUINOO data were available 1950 onwards. Monthly rainfall data from data from 1950 through 1975 were used for the Training purpose. The data from 1976 through 1990 were used for the validation purpose. The data from 1991 through 2010 were used as testing the GP models. The analysis consists of rainfall depths all over India for so called Indian Summer Monsoon season (June to September) plus the month of October.

4.0 Methodology

Genetic Programming has been used by many researchers in Hydraulics, Fluid Mechanics and Water Resources Engineering.(Babovic, 2000; Aytek and Kisi, 2008; Harris et al., 2003; Babovic and Keijzer, 2000; Baptist et al., 2007; Keijzer and Babovic, 2002; Kisi and Shiri, 2011,Babovic and Abbott, 1997a; 1997b; Giustolisi, 2004).

GP has the unique feature that it does not assume any functional form of the solution. GP can optimize both the structure of the model and its parameters. Genetic Programming evolves a computer program, relating the output and input variables. The specialty of GP approach lies with its ability to select input variables that contribute beneficially to the model and to disregard those that do not. Hence Genetic Programming is used for modeling regional rainfall prediction in this study.

GP evolves a function that relates the input information to the output information, which is of the form:

$$Y^m = f(X^n) \qquad (1)$$

Where X^n is an n-dimensional input vector and Y^m is an m-dimensional output vector.

In the proposed study, the input vector consists of Historical Average Rainfall for particular month, ENSO, EQWIN and MEI indices of three previous monthly time steps. The output vector consists of monthly rainfall for the particular month over the region.

In this work GP is implemented through Discipulus (Francone, 1998) software that is based on an extension of the originally envisaged GP called Linear Genetic Programming (LGP). Genetic programs normally represent highly non-linear solutions (Brameier and Banzhaf, 2004).

4.1 Genetic programming approach for monthly rainfall forecasting

Genetic Programming models are developed to predict Indian Summer Monsoon Rainfall. India Meteorological Department (IMD) has divided the country into five 'Homogeneous Monsoon Regions'. Hence total six separate analyses are carried out for developing six separate models of ISMR predictions. The first analysis deals with 'All India Summer Monsoon Rainfall' with India as one unit. The other five analyses deal with five 'Homogeneous Monsoon Regions' of India.

Monthly rainfall data, ENSO, EQUINOO and MEI indices from, 1950 to 2010 was used for this study. ENSO, MEI and EQUINOO indices for three immediate previous months are considered for monthly rainfall prediction.

5.0 Monthly ISMR Prediction

The analysis in this study carried out, uses the large-scale atmospheric circulation pattern ENSO, EQUINOO and MEI indices of three previous time steps for prediction of monthly rainfall. For example, for the prediction of August rainfall, ENSO, EQUINOO and MEI indices of July, June and May are given as input, with long term average rainfall August as one of the inputs. This can be treated as medium range forecast with one month lead time, which has its own importance for planning of agricultural activities and judicious management of available water in reservoirs.

Here we have tried four different combinations of predictors as:

(1) ENSO

(2) MEI

(3) ENSO + EQUINOO

(4) MEI + EQUINOO

Thus the monthly rainfall is modeled as a function of

(i) Historical average monthly rainfall of the particular month (HRt),

(ii) ENSO indices of three previous monthly time steps (EN),

(iii) MEI indices of three previous monthly time steps (MEI),

(iv) EQUINOO indices of three previous monthly time steps (EQ).

The pairs of equations for the aforesaid four combinations are listed as following:

$$R_t = f\{(HR_t)(EN_{t-3}, EN_{t-2}, EN_{t-1})\} \quad \text{.....(2)}$$

$$R_{Jun} = f\{HR_{Jun}, (EN_{March}, EN_{April}, EN_{May})\} \quad \text{.....(3)}$$

$$R_t = f\{(HR_t), (MEI_{t-3}, MEI_{t-2}, MEI_{t-1})\} \quad \text{.....(4)}$$

$$R_{Jun} = f\{(HR_{Jun}), (MEI_{March}, MEI_{April}, MEI_{May})\} \quad \text{.....(5)}$$

$$R_t = f\{(HR_t), (EN_{t-3}, EN_{t-2}, EN_{t-1})(EQ_{t-3}, EQ_{t-2}, EQ_{t-1})\} \quad \text{.....(6)}$$

$$R_{Jun} = f\{(HR_{Jun}), (EN_{March}, EN_{April}, EN_{May})(EQ_{March}, EQ_{April}, EQ_{May})\} \quad \text{.....(7)}$$

$$R_t = f\{(HR_t), (MEI_{t-3}, MEI_{t-2}, MEI_{t-1}), (EQ_{t-3}, EQ_{t-2}, EQ_{t-1})\} \quad \text{.....(8)}$$

$$R_{June} = f\{(HR_{June}), (MEI_{March}, MEI_{April}, MEI_{May}), (EQ_{March}, EQ_{April}, EQ_{May})\} \quad \text{.....(9)}$$

Thus the total summer monsoon rainfall is sum of rainfall from June through September, calculated as following.

$$R_{monsoon} = R_{June} + R_{July} + R_{August} + R_{September} \quad \text{.....(10)}$$

Where Rt stands for predicted rainfall of particular month, HR stands for Historical average of rainfall in particular month, EN stands for ENSO index, EQ stands for EQUINOO Index, MEI stands for multivariate ENSO index. The optimum number of lags to be considered for each input variables was is decided based on the 'input impacts' of that input variable during model calibration.

5.1 Results and Discussions

The analysis performed here can be treated as a real time analysis, which uses large scale atmospheric circulation pattern indices of three previous months to predict rainfall of current month. The methodology is discussed as following.

5.2 ISMR Analysis Using ENSO, EQUINOO and MEI

ISMR analysis using MEI,ENSO and EQUINOO Long term average (1950–2010) computed and used in this analysis for All India summer monsoon rainfall (June to September).

The South west monsoon normally touches Indian continent on the first day of June and returns in November. Hence rainfall in October also can be considered as a part of Monsoon rainfall activity. Monthly rainfall values during months June through October have been computed by Genetic Programming models. Monthly rainfall anomalies of observed and computed rainfall with reference to long term average (1950–2010) are also computed and presented through plots. The monthly rainfall values over Training period, validation period and Testing period for All India Summer Monsoon

Rainfall can be visualized in Figs. 5(a) and 5(b) respectively.

Three monthly time lags of ENSO, EQUINOO and MEI are considered in this analysis. It is interesting to see that the highest Correlation Coefficient in Testing of GP model for 4 combination as [ENSO], [EN+EQ],[MEI],[MEI+EQ] for monthly rainfall has been observed for 'All India Rainfall', treating India as a single unit.

This large difference in C.C. of Peninsular India region and other regions indicates that ENSO, EQUINOO and MEI indices are not able to capture the total climatic mechanism behind summer monsoon rainfall over peninsular region of India. It may be noted that ENSO, EQUINOO and MEI do not well capture rainfall mechanism during summer monsoon over peninsular India. It might be due to the fact that it is not the chief rainy season for peninsular India. The Pearson product moment Correlation Coefficients for Training, and Testing for All India and five homogeneous monsoon regions are tabulated in Table 1. Root Mean Square Error For measurement of rainfall in mm during Training and Testing are enlisted in Table 2.

Table 1 Correlation Coefficients between observed and predicted rainfall during Training and Testing

Regions	CC	ENSO	EN+EQ	MEI	MEI+EQ
All India	Training	0.936	0.942	0.938	0.932
	Testing	0.884	0.889	0.852	0.873
Central NE India	Training	0.932	0.919	0.903	0.925
	Testing	0.815	0.837	0.817	0.839
NE India	Training	0.891	0.874	0.895	0.883
	Testing	0.786	0.78	0.721	0.785
NW India	Training	0.859	0.897	0.884	0.848
	Testing	0.731	0.776	0.745	0.742
Peninsular	Training	0.773	0.806	0.635	0.724
	Testing	0.219	0.307	0.276	0.29
West Central India	Training	0.908	0.916	0.897	0.909
	Testing	0.817	0.836	0.824	0.826

Table 2 Root Mean Square Error For measurement of rainfall in mm during Training and Testing

Regions	RMSE	ENSO	EN+EQ	MEI	MEI+EQ
All India	Training	26.64	25.39	26.26	27.4
	Testing	32.79	32.21	37.3	34.24
Central NE India	Training	37.01	39.59	43.19	36.33
	Testing	60.87	57.6	60.89	57.2
NE India	Training	51.77	59.94	50.61	53.25
	Testing	67.42	67.82	77.63	67.06
NW India	Training	43.88	38.54	40.3	45.33
	Testing	52.56	48.1	51.35	51.88
Peninsular	Training	34.61	33.77	40.63	37.12
	Testing	51.56	46.31	47.33	46.6
West Central India	Training	43.62	41.647	45.73	42.77
	Testing	54.17	50.51	52.44	52.47

Graphical Presentation of Observed and Predicted of all India with (EN+EQ) combination during training and testing is shown in Fig. 2(a) and Fig. 2(b) respectively.

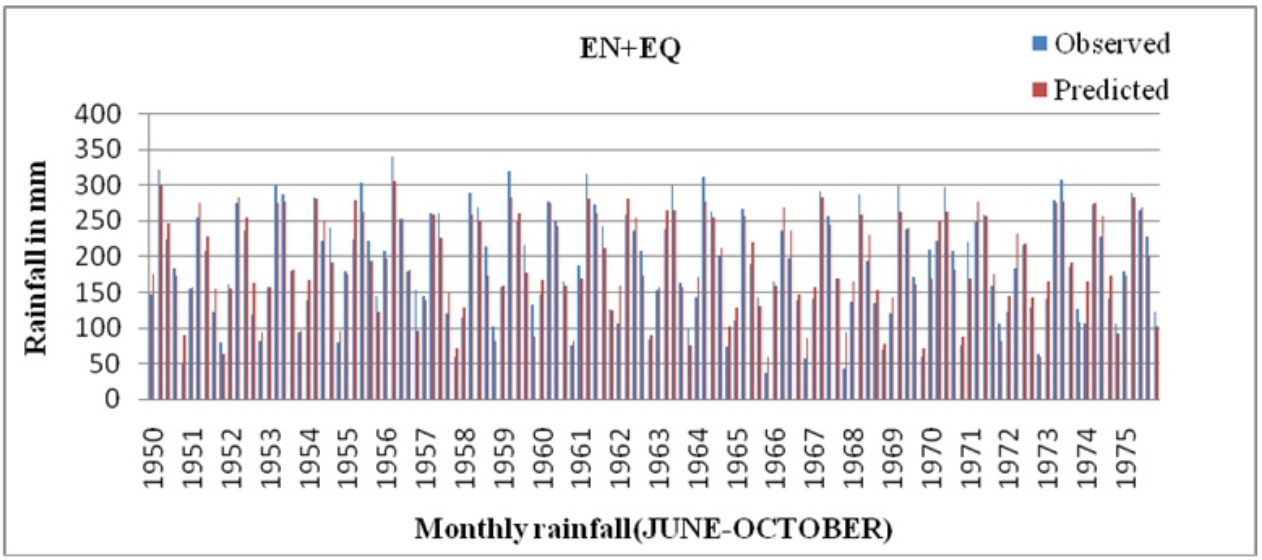

Figure 2 (a) Graphical Presentation of Observed and Predicted of all India with (EN+EQ) combination (Training)

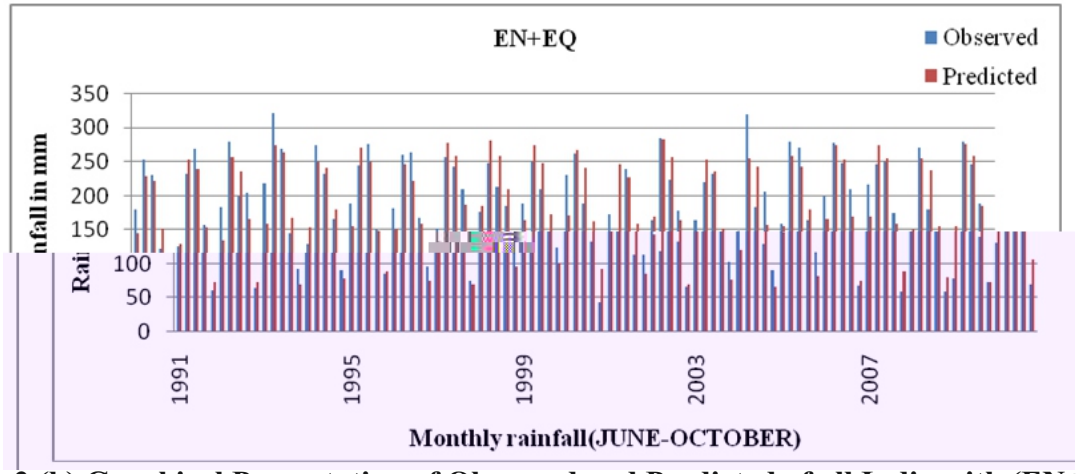

Figure 2 (b) Graphical Presentation of Observed and Predicted of all India with (EN+EQ) combination (Testing)

6.0 Conclusions

This work uses the association between the large-scale circulation patterns for prediction of Indian Summer Monsoon Rainfall over homogeneous monsoon regions of India which is quite important for Indian hydro climatology. Genetic algorithm based approach (GP), is used for the complex relationship between inputs and outputs. Various combinations of predictors viz. ENSO, EQUINOO and MEI were explored for the monthly ISMR prediction. Historical average rainfall of the particular month was invariably used in each of the Combinations. The highest correlation between observed rainfall and predicted rainfall was observed for [EN+EQ] combination for All India Rainfall. AI tool Genetic Programming developed most optimum model for prediction of Indian Summer Monsoon Rainfall with correlation coefficient between observed and predicted rainfall as good as 0.889. However considerably less correlation was observed for peninsular India, which covers Tamilnadu, Pondicherry, Coastal Andhra Pradesh, Rayalseema and South Interior Karnataka regions of India. This can be attributed to the climate systems other than ENSO, EQUINOO and MEI , which cause winter rainfall in months of November and December in south part of Peninsular India.

7.0 Selected References

1. Babovic, V., Keijzer, M., 2000. Genetic programming as a model induction engine. J. Hydroinform. 2 (1), 35–60.
2.Gadgil, S., P. N. Vinayachandran, P. A. Francis, and S. Gadgil (2004), Extremes of the Indian Summer monsoon rainfall, ENSO and equatorial Indian Ocean Oscillation, Geophys. Res. Lett., 31, L12213,.
3. Kashid and Maity (2012), Prediction of monthly rainfall on homogeneous monsoon regions of India based on large scale circulation patterns using Genetic Programming, Elsevier, Journal of Hydrology 454–455, pp. 26–41.
4.Koza JR (1992) Genetic Programming: on the programming of computers by means of natural selection. MIT Press, USAMATH
5.Parthasarathy, B., Munot, A.A., Kothawale, D.R., 1995. Monthly and Seasonal Rainfall Series for All-India Homogeneous Regions and Meteorological Subdivisions:1871–1994. IITM Research, Report No. RR-065.
6. Rasmusson E M and Carpenter T H 1983 The relationship between eastern equatorial Pacific sea surface temperatures and rainfall over India and Sri Lanka; Mon. Weather Rev. 111 517–528.
7. Sikka D R 1980 Some aspects of the large-scale fluctuations of summer monsoon rainfall over India in relation to fluctuations in the planetary and regional scale circulation parameters; Proc. Indian Acad. Sci. (Earth Planet. Sci.) 89 179–195
8. Wolter, K., 1987: The Southern Oscillation in surface circulation and climate over the tropical Atlantic, Eastern Pacific, and Indian Oceans as captured by cluster analysis. J. Climate Appl. Meteor., 26, 540-558

Effect Of Climate Change On Spatio-Temporal Distribution Of Indian Summer Monsoon Rainfall On Homogeneous Monsoon Regions Of India

S.S.Motegaonkar[1], S.S.Kashid[2]
[1]Research scholar, Walchand Institute of Technology, Solapur-413005,India.
[2]Professor at Walchand Institute of Technology, Solapur-413005. India
Email: motegaonkarshilpa@gmail.com,,sskashid@yahoo.com

A B S T R A C T

The study discusses analysis of a daily gridded rainfall data set (IMD4) at a high spatial resolution (0.25o X 0.25o, latitude X longitude) for the period of 110 years (1901-2010) over the Indian main land for assessing effect of Effect of Climate Change on Spatio-temporal Distribution of Indian Summer Monsoon Rainfall on 'Homogeneous Monsoon Regions of India'.The study presents an analysis of extreme daily rainfall (ER) events over homogeneous monsoon regions of India viz. Central India (CI), Northeast India (NEI) and West coast (WC) based on the IMD4 data set.The study covers the spatial domain of the from 6.5°N to 38.5°N in latitude(129 points), and from 66.5°E to 100°E in longitude (135 points) covering the mainland region of India (excluding the island parts). The study emphasizes re-examining results of some of the recent research studies on variability and long term trends of monsoon rainfall over India conducted using already available gridded daily rainfall data sets over the region.Thus present study focuses on Climate Change Effects on Spatio-temporal Distribution of Indian Summer Monsoon Rainfall on Homogeneous Regions of India.

The study highlights usefulness of proper water resources planning and management in the future.

Keywords:Extreme Rainfall(ER), High Rainfall(HR), Very High Rainfall(VHR), North East India(NEI), Central India(CI), Peninsular, West Coast(WC)

1. Introduction

Water is a precious natural resource and most of the water is received in the form of rainfall. Declining rainfall has adverse effect on water resources, agricultural output and economy. It is well realized that natural climate variability (e.g. decadal changes in circulation) and human induced (e.g. land cover and emissions of green house gases) changes alter the rainfall patterns. The contribution and effects of these factors are difficult to quantify and vary in time and space (IPCC, 2007). The rainfall has important socioeconomic implications over the Indian subcontinent (Fein and Stephens, 1987). Therefore it isof interest to study changing patterns of rainfall in spatio-temporal domain to identify areas undergoing rapid change.Climate change is a significant and lasting change in the statistical distribution of weather patterns over periods ranging from decades to millions of years.

The monsoon is a special phenomenon exhibiting regularity in onset and distribution within the country, but inter-annual and intrannual variations are observed. The monsoon is influenced by global and local phenomenon like El Nino, northern hemispheric temperatures, sea surface temperatures, snow cover etc.More than 22% of the world's population depends inextricably on the South Asian summer monsoon, which contributes as much as 75 percent of the total annual rainfall in major parts of the region (Dhar and Nandargi, 2003). Given the dependence of large populations on monsoon rainfall, the response of South Asian monsoon dynamics to elevated atmospheric greenhouse gas concentrations is an issue of both scientific and societal importance (Ashfaq et. al, 2009).

India Meteorological Department (IMD) has recently made three datasets available over Indian main land at different spatial grids and temporal periods. There are total two 10x10 gridded daily rainfall datasets based on fixed network of raingauge stations(Rajeevan et.al.2006,Rajeevan et.al.2008).There is a 0.50x0.50 gridded daily rainfall data set based on variable network of raingauge stations(Rajeevan et al 2009).Another daily gridded rainfall dataset of 0.250x0.250spatial resolution over Indian region was made available as a part of the larger data set developed for the monsoon Asian region under Asian Precipitation-Highly Resolved Observational Data Integration Towards Evaluation of the Water Resources Project (APHRODITE) Project(Yatagai et al, 2012).

For the present study 0.250x0.250 spatial resolution data set IMD4 is used.

The objectives of the study are-

i) To examine the variability and long term trends in the Extreme Rainfall over central India (CI) during the southwest monsoon season (June- September) using the IMD4 data, with high spatial resolution and longer period

ii) To study spatiotemporal distribution of Indian Summer Monsoon Rainfall (ISMR) and capture the changes in rainfall distribution on homogeneous monsoon regions of India.

2. Scope of Topic

Climate change is recognized as one of the major threats for the planet earth in the twenty-first century. According to the Intergovernmental Panel on Climate Change (IPCC) report (IPCC,2007), instrumental observations over the past 157 years show that temperatures at the surface have risen globally, with significant regional variations. For the global average, warming in the last (20th) century has occurred in two phases, from the 1910s to the1940s (0.35 C), and more strongly from the 1970s to the present (0.55 C).

In general, this warming intensifies the global hydrological cycle (e.g., Milly et al., 2002) and it is well established that the earth's mean surface temperature has been increasing following the last glacial maximum 21,000 years ago severe or extreme droughts at any given time during the last century.

Figure 1 shows the predicted distribution of temperature change due to global warming from Hadley CentreHadCM3climate model. These changes are based on the IS92a ("business as usual") projections of carbon dioxide and other greenhouse gas emissions during the next century, and essentially assume normal levels of economic growth and no significant steps are taken to combat global greenhouse gas emissions.

The plotted colors show predicted surface temperature changes expressed as the average prediction for 2070-2100 relative to the model's baseline temperatures in 1960-1990. The average change is 3.0°C, placing this model towards the low end of the Intergovernmental Panel on Climate Change's 1.4-5.8°C predicted climate change from 1990 to 2100. As can be expected from their lower specific heat, continents warm more rapidly than the oceans in the model with an average of 4.2°C to 2.5°C respectively. The lowest predicted warming is 0.55°C south of South America, and the highest is 9.2°C in the Arctic Ocean (points exceeding 8°C are plotted as black).(Ref-www.globalwarmingart.com)

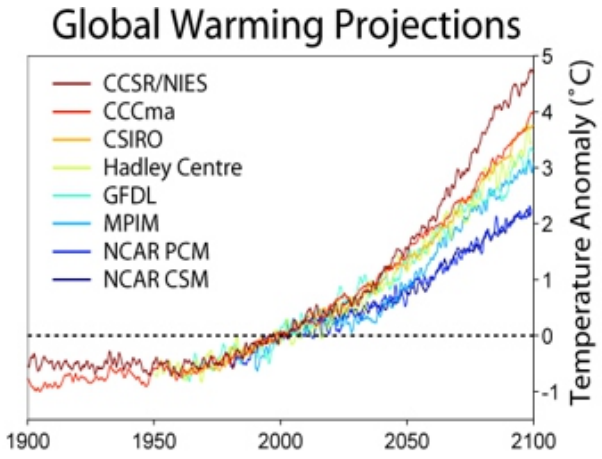

Fig. 1: Predicted Temperature changes due to Global Warming from Hadley CentreHadCM3Climate Model. (Source: www.globalwarmingart.com)

Climate change can affect crop yields (both positively and negatively), as well as the types of crops that can be grown in certain areas by impacting agricultural inputs such as water for irrigation, amounts of solar radiation that affect plant growth, etc. These changes in agricultural cloud then affect food security, trade policy, livelihood activities and water conservation issues, impacting large portions of the population in India. Hence the present work intends to study the effects of climate change on Indian Summer Monsoon Rainfall (ISMR) on 'Homogeneous Monsoon Regions of India'. Figure 2 depicts

Homogeneous Monsoon Regions of India defined by Indian Institute of Tropical Meteorology.

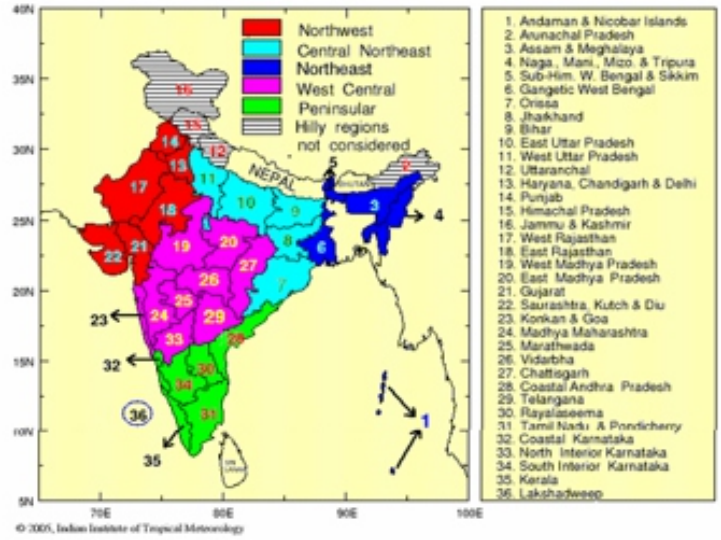

Fig. 2: 'Homogeneous Monsoon Regions of India'

(Source: Indian Institute of Tropical Meteorology)

3.Data Sources

3.1.1 Observed Rainfall Data –IMD4

The gridded rainfall data are smoother compared to individual station data. IMD4, a daily rainfall data set from the archive of National Data Centre, IMD, Pune for the period 1901-2010 were used for the present study.

The basic rainfall data and the gridded rainfall products are available from the India Meteorological Department, Pune (www.imdpune.gov.in).

The data product is based on data collected from dense network of daily rainguage data across India. Station rainfall data is converted into gridded data by spatial interpolation. The spatial domain of the IMD4 extended from 6.5°N to 38.5°N in latitude(129 points), and from 66.5°E to 100°E in longitude (135 points) covering the mainland region of India. The temporal domain of the dataset extends from 1stJanuary, 1901 to 31st December, 2010.Gridded data are also preferred for the model validations, as the model outputs are generated at fixed spatial grid points.

For the present study IMD4 data set is used as daily rainfall records from 6995 rain gauge stations from the country for the period 1901-2010 sourced from the archive of IMD were used, which is the highest ever number of stations over Indian mainland usedby any studies so far to prepare gridded rainfall over

the region. So, this data is preferably used in this study.

3.1.1 South-west Monsoon/ Indian Summer Monsoon Summer Monsoon

The SW monsoon is the most significant feature of the Indian climate. Theseason is spread over four months, but the actual period at a particular placedepends on onset and withdrawal dates. It varies from less than 75 days overWest Rajasthan, to more than 120 days over the south-western regions of thecountry contributing to about 75% of the annual rainfall.

The onset of the SW monsoon normally starts over the Kerala coast, thesouthern tip of thecountry by 1 June, advances along the Konkan coast in earlyJune and covers the whole country by middle of July.The distribution of rainfallover northern and central India depends on the path followed by thesedepressions. SW monsoon current becomes feeble and generally starts withdrawing from Rajasthan by 1st September and from north-western parts of India

3.1.2 Climate Change Variations over a Period of Time and Extreme Rainfall Events during Summer Monsoon

s and that over peninsular, east and north east India is increasing. The study was based on the daily rainfall data of about 2599 stations having at least 30 years of data during the period 1901-2005.

4.0 Methodology

For the present study, we have used an updated version of the high resolution gridded daily rainfall data developed by D.S.Pai et al (2010). The original dataset was developed for the period 1901–2010. The daily rainfall data were interpolated into grids of 0.25◦ × 0.25◦degree resolution using the interpolation Method.The grid point rainfall data at different resolutions have been used for preparing the daily rainfall over various spatial regions. The daily rainfall over a given region was computed as the area weighted rainfall over all the gridboxes over the region.Most of the analysis in this study are based on simple and well known statistical methods .GRADS (Grid Analysis and Display System) Software with graphical user interface for representation of climatic data in map.GrADS interprets station data as well as gridded data. Data from IMD4 data setis graphically overlaid, with correct spatial and time registration.

5. Results and Discussion

Monthly, seasonal and annual rainfall data over entire India as well as over homogeneousmonsoon regions of India rainfall data used for this study were collected by India Meteorological Department for a period1901-2010 and variation is observed (Refer fig.3).

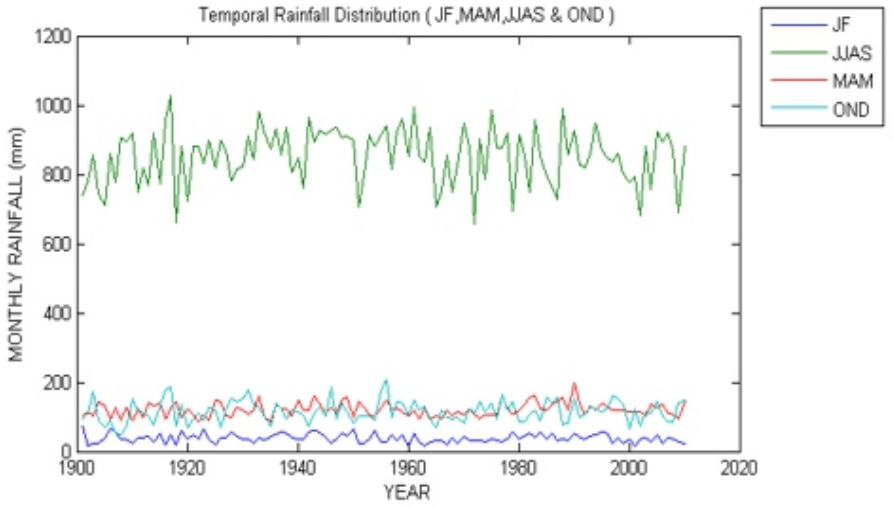

Fig 3: Variation of Monthly, seasonal, annual rainfall over Indiafor the period 1901 to 2010

The Significant increasing trends in the heavy rainfall events i.eHR (≥100 mm to 150 mm) and very heavy rainfall events i.e. VHR (≥150 mm) during the recent periods (1956-2010) were observed over Central India, whereas during the same period, the disaster potential over NEI has reduced as HR events show significant decreasing trend.

The statistical Properties of grid point extreme daily rainfall events averaged over Central India are summarized in Table 1. Whereas, the statistical Properties of grid point extreme daily rainfall events averaged over North East India are summarized in Table 2.

Table 1:Statistical Properties of grid point extreme daily rainfall events averaged over Central India

Statistical property	Categories of Extreme Rainfall	Period		
		1901-2010	1901-1955	1956-2010
Rainfall maximum at any grid (mm)		763.38	515.79	763.38
Mean (grid point events per season)	?5mm	89565	91470	87661
	5mm-100mm	88473	90426	86520
	100-150mm	834	815	852
	?150mm	259	229	290
Standard deviation (grid point events per season	?5mm	9791	9190	10083
	5mm-100mm	9771	9168	10045
	100-150mm	198	177	216
	?150mm	118	75	143
Median (grid point events per season)	?5mm	90464	93285	88425
	5mm-100mm	89398	92152	87311
	100-150mm	816	813	817
	?150mm	252	227	261

Table 2:Statistical Properties of grid point extreme daily rainfall events averaged over North East India

Statistical property	Categories of Extreme Rainfall	Period		
		1901-2010	1901-1955	1956-2010
Rainfall maximum at any grid (mm)		939.45	525.83	939.45
Mean (grid point events per season)	?5mm	26424	27267	255080
	5mm-100mm	25968	26870	25066
	100-150mm	330	309	350
	?150mm	126	88	164
Standard deviation (grid point events per season	?5mm	2225	1648	2415
	5mm-100mm	2144	1548	2286
	100-150mm	148	133	160
	?150mm	109	77	124
Median (grid point events per season)	?5mm	26797	27343	25457
	5mm-100mm	26258	26791	25066
	100-150mm	321	275	326
	?150mm	93	64	149

Mean, Standard Deviation and Median for the Grid point events for the Extreme Rainfall Events are evaluated per season for CI and NEI. During the total period (1901-2010), significant decreasing trends were observed in the MR&ER events. As a result, area weighted season rainfall also showed insignificant decreasing trend in spite of significant increasing trend in the VHR events Over India, the large scale rainfall during the SW monsoon season is received in spells with intermediate dry spells.

During the peak monsoon rainfall months (July and August) of the season, the monsoon trough shifts north and south about its normal position causing large scale intraseasonal rainfall variation over the country. The intervals of dry monsoon conditions during which the large-scale rainfall over the monsoon trough zone (the zone between which the monsoon trough fluctuates north and south wards) is interrupted for several days in July and August are known as the breaks (Ramamurthy 1969, Raghavan 1973).

Thus, the present study emphasizes use of IMD4 toexamine climatology and variability of extreme dailyrainfall events over India. During the total data period, there is decreasing trend in the MR events and increasing trends in HR events and VHR events. Over CI, the ER & MR events showed significant increasing trends in the first half and significant decreasing trend in the second half of the data period. However, the decreasing trends were observed in the ER and MR events during the total period with trend in the MR events being statistically significant.

6. Conclusions

The observation shows that the occurrence of number of Heavy Rainfall days was significantly more in the second half (1956-2010) of the data period than the first half (1901-1955). IMD4 data are also used to examine trends in the extreme rainfall (grid point rainfall of ≥ 5mm) or ER events during the southwest monsoon season over three regions over the country which were most favorable for the ER events; central India (CI), northeast India (NEI) and west coast(WC). The significant increasing trends in the HR & VHR events over CI during recent period are observed due to the increasing trend in the monsoon lows during recent decades. On the other hand, the increasing trend in the monsoon lows has opposite impact on the heavy rainfall events over NEI as the strong convergence in the low pressure systems over central India blocks the moisture supply over NEI which inhibits deep convective activity and reduces heavy rainfall events over NEI.

7. References

A K Srivastava, M Rajeevan and S R Kshirsagar, June 2008. Development of a High Resolution Daily Gridded Temperature Data Set (1969-2005) for theIndian Region,

Attri, S.D. and A. Tyagi (2010).Climate profile ofIndia. India Meteorological Department, Ministry of Earth Sciences, New Delhi: Met Monograph No.Environment Meteorology -01/2010.

BidyutBikashGoswami, Mukhopadhyay P., Mahanta R., Goswami B. N., 2010: Multiscale interaction with topography and extreme rainfall events in the northeast Indianregion; Journal of Geophysical Research, 115:D12.

Das, P.K. (1984). The monsoons – A perspective. Indian National Science Academy, New Delhi: Perspective Report Series 4.

D. S. Pai, Latha Sridhar, M. Rajeevan, O. P. Sreejith, N.S. Satbhai and B. Mukhopadyay 2013: Development and Analysis of A New High Spatial Resolution(0.25o x 0.25o) Long Period (1901-2010) Daily Gridded Rainfall Data Set Over India;NCC Research Report No. 1/2013

Gadgil, S. (2003), The Indian Monsoon and its variability, Annu. Rev. Earth. Planet.Sci., 31, 429 – 46zards,28, 1–33.

Guhathakurta P., Shreejith O. P., Menon P. A., 2011: Impact of Climate Change on extreme rainfall events and flood risk in India; J. Earth Syst. Sci.,120, No. 3, 359-373.

IPCC, Summary for Policy-makers, Climate Change 2007: Mitigation, Contribution of Working Group III to the Fourth Assessment Report of the IPCC. In B. Metz, O. R. Davidson, P.R. Bosch, R. Dave, L.A. Meyer eds. Cambridge University Press, Cambridge, United Kingdom and New York, NY, USA.

Joseph P. V. and Simon A., 2005: Weakening trend of the southwest monsoon current through peninsular India from 1950 to the present; Current Science, 89, 687-694.

K.Shashikanth, and SubimalGhosh (2013), Fine Resolution Indian Summer Monsoon Rainfall Projection with Statistical Downscaling. International Journal of Chemical, Environmental & Biological Sciences (IJCEBS) Volume 1, Issue 4 (2013) ISSN 2320-4079; EISSN 2320–4087

Krishna Kumar, K., Rupa Kumar, K., Pant, G. B., (1997). Pre-monsoon maximum and minimum temperature over India in relation to the summer monsoon rainfall; Int. J. Climatol., 17, pp. 1115–1127.

Krishnamurthy V. and Ajayamohan R. S., 2010: The composite structure ofmonsoon low pressure systems and its relation to Indian Rainfall; J.Climate, 23, 4285-4305

Krishnamurthy V. and Shukla J., 2008: Seasonal persistence and propagation ofintra-seasonal patterns over the Indian summer monsoon region; Climate Dynamics, 30,353-369.

M. Rajeevan , D. S. Pai ,R. Anil Kumar (2006), New statistical models for long-range forecasting of southwest monsoon rainfall over India

Milly, P.C.D., Wetherald, R.T., Dunne, K.A., Delworth, T.L.(2002). Increasing risk ofgreat floods in a changing climate. Nature 415, 514–517.

Parthasarathy, B., et al. (1992), Indian-summer monsoon rainfall indexes-1871– 1990, Meteorol.Mag., 121, 174– 186.

Raghavan K., 1973: Break monsoon over India; Mon. Wea. Rev. 101, 33–43.Rajeevan M., Bhate J., Kale J. D. and Lal B., 2006: High resolution daily griddedrainfall data for the Indian region: Analysis of break and active monsoon spells; Curr. Sci.91(3), 296–306
Ramamurthy K., 1969: Monsoon of India: Some aspects of the 'break' in the Indiansouthwest monsoon during July and August; Forecasting Manual 1-57 No. IV 18.3, IndiaMet. Deptt., Pune, India.
Yatagai Akiyo, Kenji Kamiguchi, Osamu Arakawa, Atsushi Hamada, NatsukoYasutomi and Akio Kitoh, 2012: APHRODITE: Constructing a Long-Term Daily GriddedPrecipitation Dataset for Asia

Study On Characterization Of Pervious Concrete For Pavements

Maniarasan.S.K[1], Nandhini.V[2], Kavin.G[3], Kavin Kumar.T.R[4]
Department of Civil Engineering, Kongu Engineering College, Perundurai, Erode - 638052
Corresponding author – Asst. Professor, Department of Civil Engineering, Kongu Engineering College
Corresponding authors – B.E., Final year students, Department of Civil Engineering, Kongu Engineering College

ABSTRACT

The project aims at studying the effect of various size of coarse aggregates, fine aggregate percentage and the use of flyash on pervious concrete and characterize the mix for use in pavements. With trials performed for determining the suitable water-cement ratio for the mixes, the proportioning was done with the help of American code for mix proportioning. Ten mixes were formulated and studied. OPC 53 grade cement, coarse aggregates of sizes 10 – 12.5 mm and 19-20 mm, fine aggregate as 5% and 10% replacement of coarse aggregate and class C flyash as 10% and 20% replacement of cement were the materials used for the study. For each mix, various material properties like compressive, tensile and flexural strength were studied. Also, the permeability through the pores was studied using the falling head permeability test. And the tile abrasion test was used to study the abrasive resistance of the concrete. The relationship between strength, permeability and porosity with the help of angularity number of aggregates has been developed. The suitability of each mix as a pavement material is studied.

Keywords: Pervious concrete, permeability, pores, abrasion

1. Introduction

The problem of water security is one of the major concerns in Indian economy today. Though India receives an abundant rainfall every year, on a global scale, due to various reasons like climatic conditions, contamination of surface waters, and manmade pressures, it mainly depends on groundwater as a source. In India groundwater accounts for 65% of irrigation water and 85% of drinking water supplies. It is estimated that 60% of ground water will be in a critical state of degradation within next 20 years. Unsustainable ground water depletion is a major issue to be addressed today. The natural ground water recharge is prevented to a large extent by the impermeable pavements laid across the country. Therefore, a solution to improve the groundwater recharge and reduce the depletion of water with the use of concrete is needed, which would be a sustainable new technology to protect our environment.[1]

Pervious concrete pavements are a unique and most cost effective means of capturing rainwater and allowing it to seep into the ground. This porous concrete is instrumental in recharging ground water and

reducing storm water runoff. The pervious concrete consists of controlled amount of cement and water in order to obtain considerable amount of paste to cover each coarse aggregate. The cementitious bond obtained between all the aggregates on tamping holds the concrete and is responsible for its strength. This concrete consists of no or less amount of fine aggregate. This omission of fines makes the concrete porous enough to allow rain water to seep through. With proper tamping and about 15% to 20% of porosity, a water permeability rate of greater than 0.34 cm/s can be achieved which supports the collection of rainwater. The main issue of pervious concrete is the development of strength for pavements. Though the strength of pervious concrete is considerably lesser than that of conventional concrete, the strength can be improved through use of optimum amount of fine aggregates, water reducers and supplementary cementitious materials (SCM).

The pervious concrete, with reduced cement content serves as a means in reducing environmental pollution, and with the use of flyash it is actually an added benefit for the same. The use of flyash in the pervious concrete not only make it economical (through cement reduction), but also serves in considerable reduction of environmental pollution.

II. Experimental Program

A. Materials and properties

Ordinary Portland Cement of grade 53 has been used as the primary binder in all the mixes and class C flyash has been used as supplementary cementitious material (SCM). Two single sized aggregates of sizes 10– 12.5 mm and 20 – 25 mm were used.

Properties	Value
Specific gravity of cement	3.15
Specific gravity of coarse aggregate (20 mm)	2.63
Specific gravity of coarse aggregate (12.5mm)	1.85
Specific gravity of fine aggregate	2.62
Water absorption of aggregate(20 mm)	2.50%
Water absorption of aggregate (12.5 mm)	2%

Table 1. Physical Properties Of Materials

In addition, a sulfonated naphthalene-formaldehyde condensate superplasticizer has been used to improve the workability of the no-slump pervious concrete mix. The properties of materials are listed in table 1.

B. Mix proportioning

The proportioning of pervious concrete was done with the help of the ACI 211.3R – 02, Guide for Selecting Proportions for No-slump Concrete. The mixes were assumed to have 15% voids and the ratio of cement to aggregate is 6, the percentage paste by volume was kept at 18%, the specific gravity, dry rodded density based on ASTM C 29/ C29M and water absorption of the aggregates were determined and the proportioning was done at saturated surface dry condition (SSD). By the ACI recommendations, dry-rodded volume of coarse aggregate in a unit volume of concrete is used in the proportioning of the pervious concrete. The volume varies with the percentage of fine aggregate substituted, that is, the volume of the coarse aggregate is reduced with the increase in fine aggregate percentage based on the dry-rodded density tests made by the National Aggregates Association- National Ready Mixed Concrete Association (NAA-NRMCA).

3 trial mixes were cast with water cement ratio of 0.30, 0.33 and 0.35 and checked for compressive strengths.

In a conventional concrete, with the reduction of w/c ratio, the strength of the concrete improves. It was found the water cement ratio does not have the same effect on strength of concrete as that of the conventional concrete. The mix with 0.33 w/c ratio gave the required 7 day compressive strength 7.35 N/mm2 with the required workability for the usually dry mix.

The table 2 and 3 gives the details of mix proportioning done.

Fines	Flyash	SP	20-25 mm	10-12.5mm
0	0	0	M1F0	M2F0
5	0	0	M1F05	M2F05
10	0	0	M1F10	M2F10
0	10	0.2	M1FA10	M2FA10
0	20	0.3	M1FA20	M2FA20

C. Preparation and testing of specimens

Compressive strength tests:

Compressive strength tests were performed in accordance with IS 516. Specimens of size 150 X 150 X 150 mm cubes were cast for all the mixes. After 24 hours of casting, the specimens were demoulded and subjected to curing till the day of testing. The testing was done at 3, 7 and 28 days to assess the variation of strength of pervious concrete with age.

Tensile strength test of specimen:

The tensile strength was assessed with the split tensile strength value, the test performed in accordance to IS 5816. Cylindrical specimens of size 150 mm in diameter and 300 mm in height were cast for each mix and were tested by applying compressive line load along the horizontal axis of the cylinder. The specimens were subjected to curing and were tested at 7 day and 28 day.

Flexural strength test of specimen:

The third point loading flexural strength test was done to assess the flexural strength of specimens of all the mixes. Beam specimens of size 100 X 100 X 300 mm were cast and tested in accordance to IS 516. The specimens were tested at 7 days and 28 days after curing.

Permeability test:

The permeability rate of water through all the pervious concrete specimens was found using the falling head permeability test. Cubical specimens of size 150 X 150 X 150 mm were cast and the permeability test was done. The specimens were tested at 28 day after subjected to curing. The rate of permeability was found using,

$$k = \frac{aL}{At} \ln \frac{h_1}{h_2}$$

Where a is the area of the pipe, A is the area of the specimen, L is the thickness of specimen, t is time in seconds, h1 and h2 are the head differences in water.

Abrasion resistance:

The abrasion resistance of concrete specimens was found using tile abrasion test done on tile specimens of size 50 X 50 X 20 mm. The specimens were tested at 28 day after curing in the Aimil Dorry Abrasion Test Machine.

Angularity number:

The angularity number is a parameter for relating the shape of the aggregate with the porosity. The test was done in accordance with IS 2386 (Part I). The angularity number was found by compacting the aggregates in a cylinder of known volume. The aggregates in the cylinder were subjected to 100 blows by tamping rod at the rate of 2 blows per second, such that the blows were evenly distributed. The volume of the cylinder was found by weighing the amount of water required to fill in the cylinder.

			Cementitious Materials				
Mix ID	Aggregates(Kg)	Fines(Kg)	Total (Kg)	OPC(%)	Flyash(%)	SP(%)	w/c
M1F0	1700	-	278.21	100	-	-	0.33
M2F0	1700	-	278.21	100	-		0.33
M1F05	1600	80	278.21	100	-	0.8	0.33
M2F05	1600	80	278.21	100	-		0.33
M1F10	1550	155	278.21	100	-	0.2	0.33
M2F10	1550	155	278.21	100	-	-	0.33
M1FA10	1700	-	278.21	90	10	0.8	0.33
M2FA10	1700	-	278.21	90	10	0.8	0.33
M1FA20	1700	-	278.21	80	20	0.8	0.33
M2FA20	1700	-	278.21	80	20	0.8	0.33

Table 3.mix Proportions Per 1 m^3 Of Pervious Concrete

The angularity number was found by,

Angularity number $= 67 - \frac{100\,W}{C\,G_A}$

Where, W is mean weight in g of aggregate in the cylinder, C is weight of water in g required to fill in the cylinder, GA is the specific gravity of the aggregates.

The number 67 indicates that 33% of porosity is present by default in the compacted aggregates. Hence if the angularity number 0, it indicates a porosity of 33%

III. Results And Discussions

A. Porosity

The porosity of the pervious concrete was analyzed with the help of angularity number of the two sizes of aggregates used. The angularity number gives the porosity present in the aggregates after compaction. It was related to the porosity of each concrete mix found. The bulk volume and the volume of solids were determined to find the porosity. The volume of solids was found using the difference between mass of the

sample in air and mass of the submerged sample. The porosity was found using,

$$\text{Porosity \%} = \frac{\text{Volume of solids}}{\text{Bulk volume}} \text{ X } 100$$

Mix details	Aggregate size	Value
M1	20-25 mm	4
M2	10-12.5 mm	0

Table 4. Angularity Number Of Aggregate In Each Mix

The angularity number for mixes is given in table 4 and the effect of angularity number on the porosity of concrete is shown in table 5.

It could be found that no distinct effect of angularity on porosity was found. But it is clear from the results that addition of fine aggregate to the concrete, makes the concrete less porous and hence the mix with an angularity number of 0 and 10% fines addition had the low porosity. The porosity was within a range of 25- 40% which is acceptable.

S.NO	Mix details	Angularity number	Porosity %
1	M1F0	4	37
2	M2F0	0	35
3	M1F05	4	33
4	M2F05	0	32
5	M1F10	4	30
6	M2F10	0	29
7	M1FA10	4	38
8	M2FA10	0	37
9	M1FA20	4	36
10	M2FA20	0	36

Table 5. Effect Of Angularity Number On Porosity Of Concrete

B. Strength characteristics

The compressive strength shown in tables 6 and 7 gives the mean compressive strength of 3 identical

cube specimens, tested on the same age. Noticeable strength variations were seen among the specimens. The compressive strength of the control mixes without any fines or flyash addition showed almost same trend in strength development. But it was found that with the reduction of aggregate size, the compressive strength of the concrete increased. This was because, with the reduction in size of aggregates the surface area increased and also the paste contact area increased leading to a good bond between the aggregates. Also with the reduction in size of aggregates, the voids in the aggregates reduced leading to a better compressive strength.

Mix details	Compressive strength (N/mm^2)			Split tensile strength (N/mm^2)	Flexural strength (N/mm^2)
	3 day	7 day	28 day	28 day	28 day
M1F0	5.78	16.2	23.2	3.68	2.6
M2F0	5.91	15	24	3.81	2.8

Table 6. Strength Characteristics Of The Control Mixes With Respect To Age

		Compressive strength (N/mm^2)		
S.NO	Mix details	3 days	7 days	28 days
1	M1F0	5.78	16.2	23.2
2	M2F0	5.91	15	24
3	M1F05	5.8	17.4	27
4	M2F05	5.92	16.2	27.5
5	M1F10	4.89	18.2	29.5
6	M2F10	5.1	18	30.1
7	M1FA10	4.56	14.3	21.2
8	M2FA10	4.3	16.2	22.1
9	M1FA20	4.62	10.5	21
10	M2FA20	4.52	9.6	20

Table 7. Compressive Strength Of Pervious Concrete At Various Stages

The addition of fines greatly improved the compressive strength of concrete. This was mainly because of the reduction in porosity with addition of fines. The use of flyash as supplementary cementitious replacement did not affect the strength of the concrete. Although a % reduction of strength was observed.

With the results, it was observed that pervious concrete with reasonable strength as that of control mixes can be obtained with flyash usage.

The results show that, there has been 30% of increase in strength from 7 day to 28 day in the control mixes and with 10% flyash replacement, whereas, there has been 50% increase in case of 20% flyash replacement.

The strength characteristics of the control mixes with respect to the age is mentioned in table 6. The compressive strength, split tensile strength and flexural strength test of all the mixes are listed in table 7, table 8 and table 9 respectively.

The tensile strength results from table 8 shows that the pervious concrete mixes were really weak in tension. It showed the same trend in strength development as that of the compressive strength. With the addition of fines there has been a slight improvement in the tensile strength of the concrete.

		Tensile strength (N/mm^2)	
S.NO	Mix details	7 days	28 days
1	M1F0	0.509	3.68
2	M2F0	0.61	3.81
3	M1F05	0.52	3.82
4	M2F05	0.65	3.82
5	M1F10	0.53	3.96
6	M2F10	0.6	4
7	M1FA10	0.42	3.31
8	M2FA10	0.45	3.29
9	M1FA20	0.4	2.96
10	M2FA20	0.43	3

Table 8. Tensile Strength Of Pervious Concrete At Various Stages

		Flexural strength (N/mm^2)	
S.NO	Mix details	7 days	28 days
1	M1F0	0.14	2.6
2	M2F0	0.14	2.8
3	M1F05	0.28	3.3
4	M2F05	0.28	3
5	M1F10	0.28	3.5
6	M2F10	0.28	3.9
7	M1FA10	0.14	2.5
8	M2FA10	0.14	2.6
9	M1FA20	0.14	2.4
10	M2FA20	0.14	2.4

Table 9. Flexural Strength Of Pervious Concrete At Various Stages

The flexural strength of pervious concrete is very less compared to the conventional concrete owing to the porosity. The results from table 9 show that the flexural strength actually increased with the reduction of porosity. And the porosity was reduced with the addition of fine aggregate into the mix and also the reduction in size of the aggregate. Hence the mix with aggregates of size 10-12.5 mm and 10 % fines addition exhibited higher flexural strength.

C. Permeabiltiy

The rate of water permeability through each of the concrete specimen was found using falling head permeability test. The results showed that addition of fine aggregate to the mix, resulted in considerable reduction of permeability of water. With the addition of fines, the strength greatly improved because of reduction of voids which further resulted in the reduction of water permeability rate. The porosity had a considerable effect on the rate of permeability. With the decrease in size of aggregate, the coefficient of permeability also decreased. This was mainly because of the reduction in the porosity of the mix. Table 11 shows the variation of average permeability rate with the variation of size of aggregates. The replacement of cement with flyash did not have considerable effect on permeability. A suitable permeability rate was achievable. Therefore, the mixes with higher porosity showed higher permeability rate. Table 10 shows the permeability rate of each mix.

D. Abrasion

Abrasion is a major factor when it comes to pavement application. Each specimen was tested using the tile abrasion test. As the results in table 12 shows, the abrasion in terms of weight loss % reduced with the reduction in size of aggregates. This becomes evident with M1F0 and M2F0 mixes. This is mainly because, with the reduction of aggregate size, the bond between the aggregates is comparatively high and hence lesser abrasion.

The effect of fine aggregate addition and flyash substitution on abrasion turned out inconclusive. Also, there was difficulty in preparing the right size of tile specimen for the test, owing to the requirement of smaller size. Hence, it was evident that tile abrasion test is not suitable to study the abrasion effect on fine aggregate addition or flyash replacement in pervious concrete.

S.NO	Mix details	Permeability (cm/sec)
1	M1F0	1.23
2	M2F0	1.1
3	M1F05	1.15
4	M2F05	0.99
5	M1F10	0.98
6	M2F10	0.91
7	M1FA10	1.3
8	M2FA10	1.26
9	M1FA20	1.26
10	M2FA20	1.23

Table 10. Water Permeability Rate Of Pervious Concrete

S.NO	Size of aggrega tes	Mix ID	Permea bility rate (cm/sec)
1	20 – 25 mm	M1F0,M1F05,M1F10,M 1FA10,M1FA20	1.18
2	10 – 12.5 mm	M2F0,M2F05,M2F10,M 2FA10,M2FA20	1.09

Table 11. Variation Of Permeability Rate With Size Of Aggregates

S.NO	Mix details	Abrasion %
1	M1F0	4.2
2	M2F0	4
3	M1F05	4.47
4	M2F05	4.2
5	M1F10	4.43
6	M2F10	4.56
7	M1FA10	4
8	M2FA10	4.45
9	M1FA20	4.45
10	M2FA20	4.23

Table 12. Abrasion Resistance Of Pervious Concrete

E. Effect of percentage of fines on strength characteristics

The fine aggregate addition into the mix, by replacement of some percentage of coarse aggregate led to reduction in porosity of the concrete. Hence there was significant improvement in the strength characteristics of the concrete. All compressive, tensile and flexural strength of concrete improved with addition of fine aggregate.

This is clearly indicated by the graph plotted between porosity and strength characteristics as shown in Fig 1

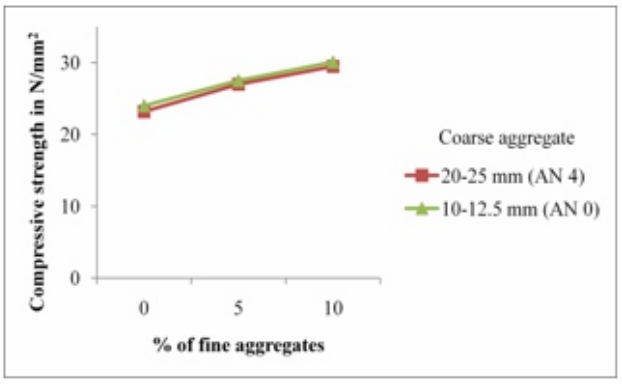

Fig 1 Relationship Between % Of Fines And Compressive Strength (n/mm^2)

F. Effect of porosity on permeability and strength characteristics

It was stated earlier that with the reduction in porosity, that is, with reduction in voids, the strength of the concrete is increased. This is mainly because, with the reduction in the porosity of the concrete, the density of the concrete is increased. This leads to concrete with greater strength and durability. This is justified by the plotted graph shown in Fig 2.

Also, if the porosity is more, naturally the flow of water also will be more. And hence the rate of water permeability through the concrete specimens will be quite high. With the reduction in porosity, the water permeability rate also got reduced. This is justified by the graph plotted between the porosity of each mix and the water permeability rate as shown in Fig 3

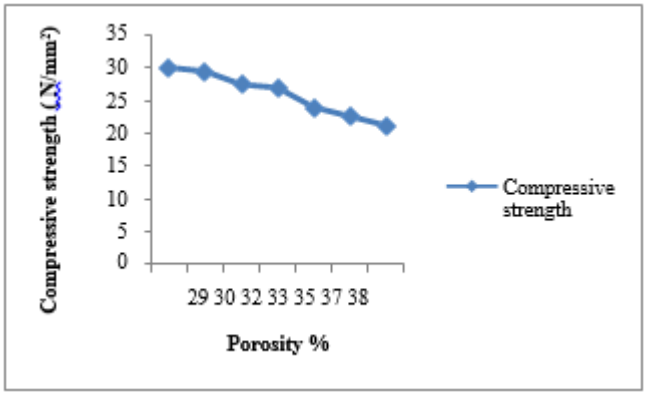

Fig 2. Relationship Between Porosity (%) And Compressive Strength (n/mm^2)

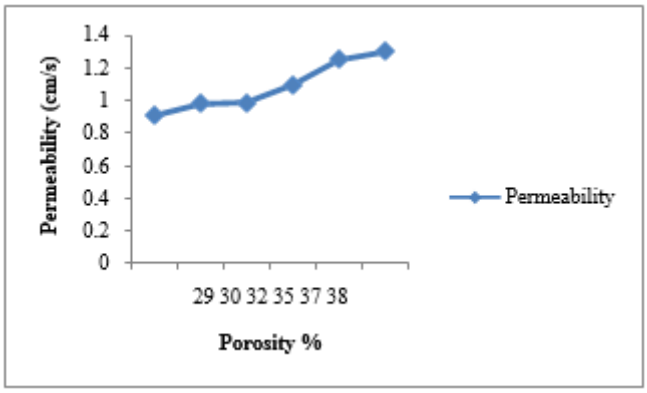

Fig 3. Relationship Between Porosity (%) And Permeability Rate (cm/s)

G. Effect of age and flyash content on strength characteristics

Flyash was used as supplementary cementitious material (as replacement of part of cement) mainly to improve the performance of the concrete and study its effect on strength characteristics. From the graph plotted, as shown in Fig 4 and Fig 5, it can be seen that the compressive strength of concrete with flyash gained lesser compressive strength than conventional pervious concrete. It was observed that the main reason for this is lesser bond strength than the strength a cement bond could offer. The variation of

percentage of flyash did not have much effect on the compressive strength. The increase in flyash percentage from 10% to 20% gave similar compressive strength results.

The development of strength from 3 day to 7 day was comparatively slower for flyash replaced concrete than that of the conventional concrete. This is the pozzolonic character of flyash showing slower strength development in the beginning.

With variation in size of the aggregates, for 10% flyash replacement the same trend as that of the control mix was observed. That is, there was improvement of strength with decrease in size of aggregate from 20-25 mm to 10-12.5 mm.

The same trend was observed with tensile strength development in terms of age and flyash content.

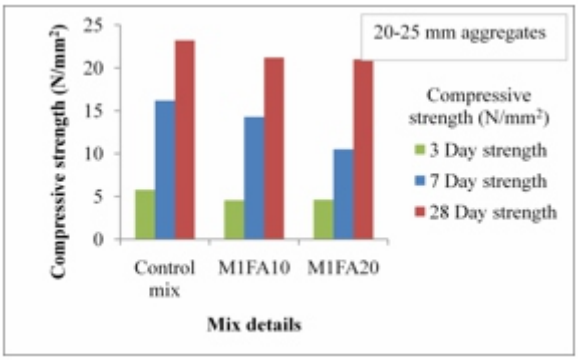

Fig 4. Effect Of Flyash On Compressive Strength (20-25 Mm)

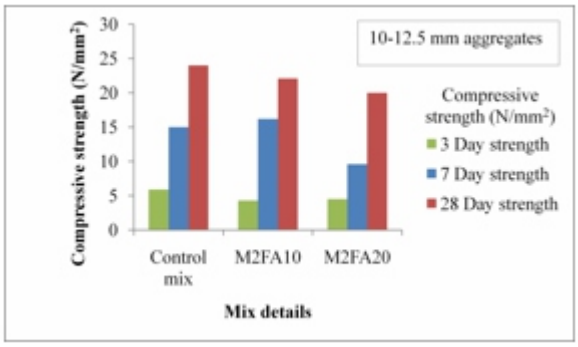

Fig 5. Effect Of Flyash On Compressive Strength (10-12.5 Mm)

H. Effect of flyash content and size of aggregate on porosity and permeability

The concrete mix with flyash replacement of 10% exhibited greater porosity of 38% and hence a greater permeability rate of 1.3cm/s than the conventional control mix and the concrete with 20% flyash replacement. It is represented in Fig 6 and Fig 7.

The concrete with larger size aggregates of 20-25 mm exhibited greater porosity and permeability rate. And the concrete with flyash replacement of 10% (20-25 mm) exhibited greater porosity and permeability than that of the control mix and concrete with 20% flyash replacement

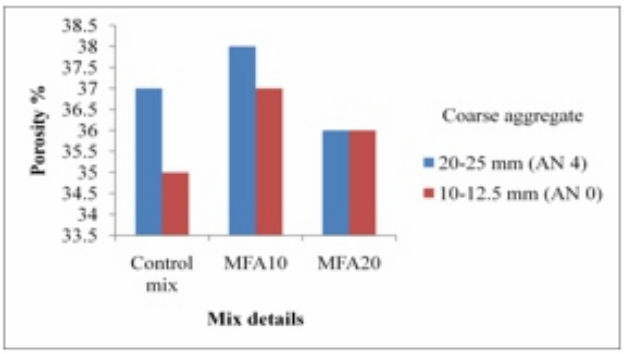

Fig 6. Effect Of Flyash And Size Of Aggregate On Porosity

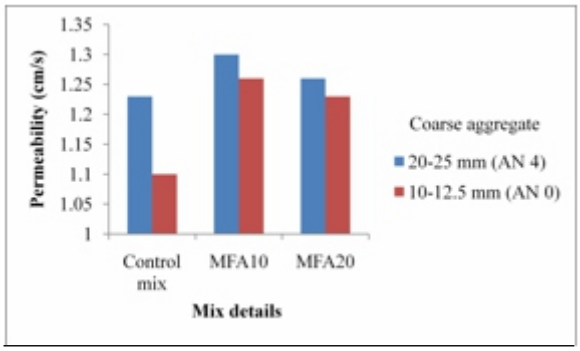

Fig 7. Effect Of Flyash And Size Of Aggregates On Permeability

I. Effect of fine aggregate and size of aggregate on porosity and permeability

The addition of fine aggregate content in the concrete led to reduction in voids due to greater surface area and hence a greater bond strength. This led to a reduction in porosity and hence the mix without any fines addition exhibited a greater porosity. Similarly, the reduction of size of aggregates also led to reduction in voids and hence mix with larger size aggregate exhibited a greater porosity of 37% as shown in Fig 8.

This had a similar effect on water permeability rate. The mix with no fine aggregate addition and greater aggregate size (20-25 mm) had a greater water permeability rate of 1.23 cm/s as shown in Fig 9.

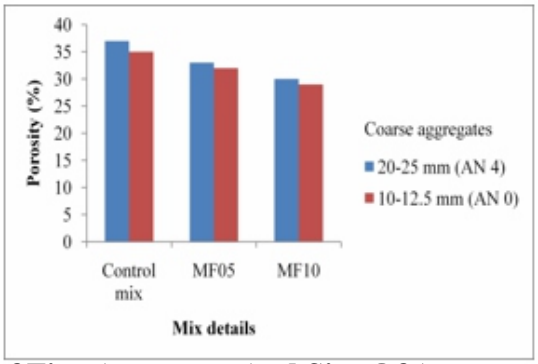

Fig 8. Effect Of Fine Aggregate And Size Of Aggregate On Porosity

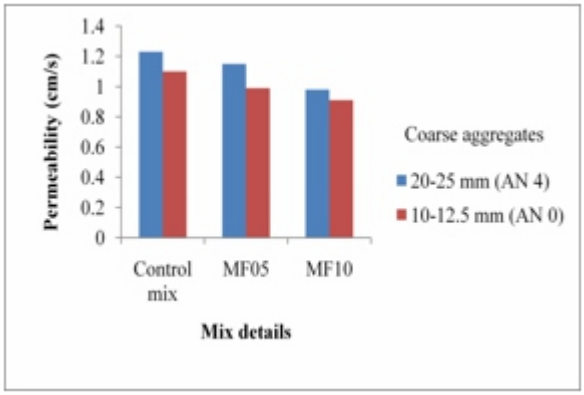

Fig 9. Effect Of Fine Aggregate And Size Of Aggregate On Permeability

J. Mix with suitability for application on pavements

For the application of pervious concrete in pavements, there is a requirement of good strength. It was found earlier that reduction in size of aggregates and addition of fines yielded good results. The graphs plotted in Fig 10, Fig 11 and Fig 12 shows the mix with greater compressive, tensile and flexural strength. The mix with aggregate size of 10-12.5 mm and coarse aggregate replacement of 10% by fines has achieved the maximum strength of 30.1 MPa in compression, which is suitable for pavement application.

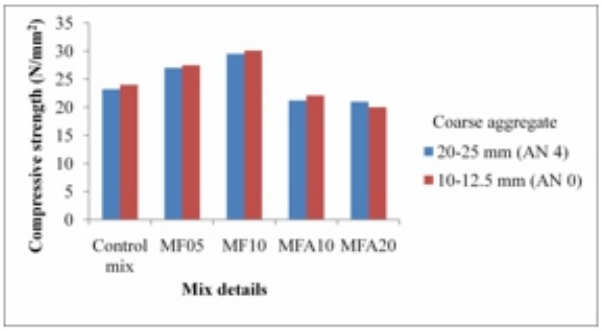

Fig 10. Comparison Of Compressive Strength Of All Mixes

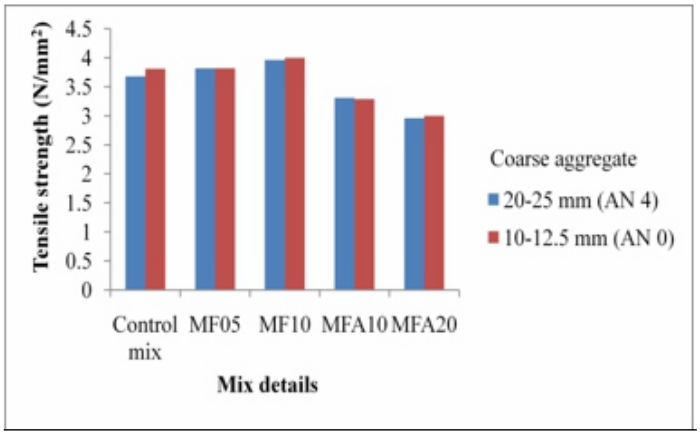

Fig 11. Comparison Of Tensile Strength Of All Mixes

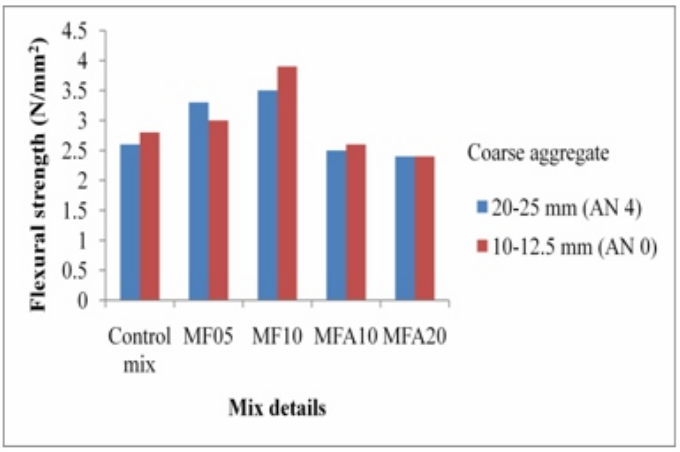

FIG 12. COMPARISON OF FLEXURAL STRENGTH OF ALL MIXES

IV. Conclusion

The main objective of the project was to develop a suitable mix for pavement application. Hence in order to improve the strength of the concrete Class C flyash was used as partial cement replacement. It was found that with the addition of flyash, the mix yielded lower strength than that of conventional pervious concrete, mainly because of lower bond strength. Hence fine aggregate was added to the concrete mix for strength improvement. But it yielded lesser water permeability rate. Hence fine aggregate was added to the mix in the form of coarse aggregate replacement.

Also, the variation of strength with size of the aggregate was also studied. It was found that fine aggregate replacement of 10% of coarse aggregate of size 10-12.5 mm yielded the maximum strength, suitable for pavement application. This mix had the needed porosity of 29% and a water permeability rate of cm/s suitable for proper drainage of runoff water on pavements.

Although the flyash addition into the mix didn't yield the needed results for pavement application, it yielded strength comparable to that of conventional control mixes and it shows suitability towards other application of pervious concrete on pathways etc. It paves a way for sustainable pervious concrete applications which calls for future study.

V . Refernces

- *ACI 211.3R-02, 'Guide for selecting proportion for no-slump concrete'*
- *ASTM C29/C 29 M – 97 , 'Standard method of test for bulk density and voids in concrete'*
- *Baoshan Huang, Hao Wu, Xiang Shu, Edwin G. Burdette (2010) , 'Laboratory Evaluation of permeability and strength of polymer modified pervious concrete'*
- *Darshan S. Shah, Prof. Jayeshkumar Pitroda, Prof. J.J. Bhavsar (2013), 'Pervious concrete: New era for rural road pavement', International Journal of Engineering Trends and Technology, Vol 4 issue 8*
- *Dale.P.Bentz (2008), 'Virtual pervious concrete: microstructure, percolation, and permeability', ACI Materials Journal, title no. 105 – M35*
- *IS 2386(Part III) – 1963, 'Indian Standards methods of test for aggregates for concrete'*

Instructions for Authors

Essentials for Publishing in this Journal

1 Submitted articles should not have been previously published or be currently under consideration for publication elsewhere.

2 Conference papers may only be submitted if the paper has been completely re-written (taken to mean more than 50%) and the author has cleared any necessary permission with the copyright owner if it has been previously copyrighted.

3 All our articles are refereed through a double-blind process.

4 All authors must declare they have read and agreed to the content of the submitted article and must sign a declaration correspond to the originality of the article.

Submission Process

All articles for this journal must be submitted using our online submissions system. http://enrichedpub.com/ . Please use the Submit Your Article link in the Author Service area.

Manuscript Guidelines

The instructions to authors about the article preparation for publication in the Manuscripts are submitted online, through the e-Ur (Electronic editing) system, developed by **Enriched Publications Pvt. Ltd**. The article should contain the abstract with keywords, introduction, body, conclusion, references and the summary in English language (without heading and subheading enumeration). The article length should not exceed 16 pages of A4 paper format.

Title

The title should be informative. It is in both Journal's and author's best interest to use terms suitable. For indexing and word search. If there are no such terms in the title, the author is strongly advised to add a subtitle. The title should be given in English as well. The titles precede the abstract and the summary in an appropriate language.

Letterhead Title

The letterhead title is given at a top of each page for easier identification of article copies in an Electronic form in particular. It contains the author's surname and first name initial .article title, journal title and collation (year, volume, and issue, first and last page). The journal and article titles can be given in a shortened form.

Author's Name

Full name(s) of author(s) should be used. It is advisable to give the middle initial. Names are given in their original form.

Contact Details

The postal address or the e-mail address of the author (usually of the first one if there are more Authors) is given in the footnote at the bottom of the first page.

Type of Articles

Classification of articles is a duty of the editorial staff and is of special importance. Referees and the members of the editorial staff, or section editors, can propose a category, but the editor-in-chief has the sole responsibility for their classification. Journal articles are classified as follows:

Scientific articles:

1. Original scientific paper (giving the previously unpublished results of the author's own research based on management methods).

2. Survey paper (giving an original, detailed and critical view of a research problem or an area to which the author has made a contribution visible through his self-citation);

3. Short or preliminary communication (original management paper of full format but of a smaller extent or of a preliminary character);

4. Scientific critique or forum (discussion on a particular scientific topic, based exclusively on management argumentation) and commentaries. Exceptionally, in particular areas, a scientific paper in the Journal can be in a form of a monograph or a critical edition of scientific data (historical, archival, lexicographic, bibliographic, data survey, etc.) which were unknown or hardly accessible for scientific research.

Professional articles:

1. Professional paper (contribution offering experience useful for improvement of professional practice but not necessarily based on scientific methods);
2. Informative contribution (editorial, commentary, etc.);
3. Review (of a book, software, case study, scientific event, etc.)

Language

The article should be in English. The grammar and style of the article should be of good quality. The systematized text should be without abbreviations (except standard ones). All measurements must be in SI units. The sequence of formulae is denoted in Arabic numerals in parentheses on the right-hand side.

Abstract and Summary

An abstract is a concise informative presentation of the article content for fast and accurate Evaluation of its relevance. It is both in the Editorial Office's and the author's best interest for an abstract to contain terms often used for indexing and article search. The abstract describes the purpose of the study and the methods, outlines the findings and state the conclusions. A 100- to 250-Word abstract should be placed between the title and the keywords with the body text to follow. Besides an abstract are advised to have a summary in English, at the end of the article, after the Reference list. The summary should be structured and long up to 1/10 of the article length (it is more extensive than the abstract).

Keywords

Keywords are terms or phrases showing adequately the article content for indexing and search purposes. They should be allocated heaving in mind widely accepted international sources (index, dictionary or thesaurus), such as the Web of Science keyword list for science in general. The higher their usage frequency is the better. Up to 10 keywords immediately follow the abstract and the summary, in respective languages.

Acknowledgements

The name and the number of the project or programmed within which the article was realized is given in a separate note at the bottom of the first page together with the name of the institution which financially supported the project or programmed.

Tables and Illustrations

All the captions should be in the original language as well as in English, together with the texts in illustrations if possible. Tables are typed in the same style as the text and are denoted by numerals at the top. Photographs and drawings, placed appropriately in the text, should be clear, precise and suitable for reproduction. Drawings should be created in Word or Corel.

Citation in the Text

Citation in the text must be uniform. When citing references in the text, use the reference number set in square brackets from the Reference list at the end of the article.

Footnotes

Footnotes are given at the bottom of the page with the text they refer to. They can contain less relevant details, additional explanations or used sources (e.g. scientific material, manuals). They cannot replace the cited literature.
The article should be accompanied with a cover letter with the information about the author(s): surname, middle initial, first name, and citizen personal number, rank, title, e-mail address, and affiliation address, home address including municipality, phone number in the office and at home (or a mobile phone number). The cover letter should state the type of the article and tell which illustrations are original and which are not.